UNIVERZA V LJUBLJANI

FAKULTETA ZA FARMACIJO

JANA KOVAČ

MAGISTRSKA NALOGA

ENOVITI MAGISTRSKI ŠTUDIJ FARMACIJE

Ljubljana, 2014

UNIVERSITY OF LJUBLJANA

FACULTY OF PHARMACY

JANA KOVAČ

SYNTHESIS, CHARACTERIZATION AND FRAGMENTATION OF QUATERNARY AMMONIUM PALMITOYL GLYCOL CHITOSAN

SINTEZA, VREDNOTENJE IN FRAGMENTACIJA DERIVATA ETILENGLIKOL HITOSANA

Ljubljana, 2014

Magistrsko nalogo sem opravljala na Fakulteti za farmacijo pod mentorstvom Prof. Dr. Janka Kosa in somentorstvom Prof. Andreasa G. Schatzleina.

Spektroskopske meritve, kromatografske metode, TEM mikroskopijo in druga merjenja smo opravili na School of Pharmacy, University College London, Združeno kraljestvo.

Zahvala

Zahvalo namenjam vsem, ki so sodelovali pri nastanku te magistrske naloge, predvsem pa svojemu somentorju Prof. Andreasu G. Schatzleinu, Prof. Ijeomi Uchegbu in Dr. Antoniu Iannitelli iz UCL School of Pharmacy. Zahvaljujem se svojemu mentorju Dr. Janku Kosu, za vso pomoč in usmerjanje pri pisanju naloge. Svojim bližnjim se zahvaljujem za vsestransko podporo tekom študija. Ne nazadnje bi se rada zahvalila svojim prijateljem in sošolcem, za lepe spomine in nepozabna študentska leta.

Acknowledgement

I would like to thank everyone who has contributed to this thesis. First, I would like to thank my lab group at UCL School of Pharmacy for the opportunity, help and unforgettable six months, especially to Prof. Andreas G. Schatzlein, Prof. Ijeoma Uchegbu and Dr. Antonio Iannitelli. Next, I would like to thank Prof. Dr. Janko Kos for his help and guidance. Last but not least, I would like to sincerely thank my family, especially my parents, for their unconditional love and support all along. To my friends and classmates, for lifelong memories and unforgettable college years.

Izjava

Izjavljam, da sem magistrsko nalogo samostojno izdelala pod mentorstvom prof. Dr. Janka Kosa in somentorstvom Prof. Andreasa G. Schatzleina.

Ljubljana, 2014 Jana Kovač

Predsednik komisije: izr. prof. Dr. Marko Anderluh, mag. farm.

Članica komisije: doc. Dr. Nataša Karas Kuželički, mag. farm.

Table of content

Table of figures

Abstract

Because of its acceptability, convenience, low cost and good patient compliance, oral route of application is still the most popular way of drug delivery. Good permeability across intestinal membrane, good solubility in gastrointestinal fluids and stability in gastrointestinal tract are the optimal conditions for oral administration of a drug. There are different approaches to achieve these demands and encapsulation of a drug inside nanoparticles is among the most popular. Nanoparticles enhance solubility, reduce toxicity, enable sustained release of the drug, increase enzymatic and physical stability of the drug, enhance the transport across different biological barriers and target the drug delivery to a specific site in the body.

Chitosan is a natural cationic polymer, obtained by deacetylation of chitin, which has different applications in Pharmacy. Nanoparticles of chitosan derivatives, such as GCPQ, self-assemble to form micelles and have shown great potential as a delivery system, due to their positive effects on absorption and bioavailability of hydrophobic and also hydrophilic drugs. Being biocompatible, biodegradable and non-toxic, they are being widely researched. Their efficacy of the polymer has been confirmed for both oral and intravenous delivery route in drug delivery studies, whiles the mechanism by which it is taken into the tissues, is still being a subject of research.

The structure and characteristics of GCPQ have not been completely elucidated yet and demand further research, however the high molecular weight of GCPQ does not allow the use of usual spectroscopic methods. Fragmentation of the polymer, applying suitable method, would result in formation of fragments, small enough to be analysed by spectroscopic methods. The main focus of my master thesis has been searching, applying and optimizing fragmentation method of GCPQ and analysis of fragmentation results. The remaining part of the thesis was dedicated to the synthesis and characterization of polymers with desired characteristics, which have subsequently been used to form nanoparticles in different solvents with an aim to evaluate solvents' and polymers' characteristics impact on nanoparticles formation and size.

Key words: chitosan, GCPQ, nanoparticles, MALDI TOF, fragmentation

Povzetek

Peroralna aplikacija je najbolj razširjen način aplikacije zdravil, zaradi svoje neinvazivnosti, dobre kompliance, priročnosti in nizkih stroškov. Pogoj za peroralno aplikacijo učinkovine je med drugim njena dobra absorpcija preko gastrointestinalne membrane, pa tudi dobra topnost in fizikalna stabilnost v prebavilih. Obstajajo različni pristopi za izboljšanje biološke uporabnosti po peroralni aplikaciji, med katerimi je trenutno v središču pozornosti priprava nanodelcev z učinkovino. Nanodelci omogočajo izboljšanje topnosti, zmanjšanje toksičnosti, podaljšano sproščanje, povečanje encimske in fizikalne stabilnosti učinkovine in povečanje transporta učinkovine čez biološke membrane ter ciljano dostavo učinkovine v organizmu.

Hitosan je naravni kationski polimer s številnimi aplikacijami v farmaciji, pridobljen z deacetilacijo hitina. Nanodelci derivatov hitosana, kot je tudi GCPQ, v mediju tvorijo micele in imajo zaradi dokazanih ugodnih učinkov na absorpcijo in biološko uporabnost hidrofobnih, pa tudi hidrofilnih učinkovin velik potencial kot dostavni sistem. Biokompatibilnost, biorazgradljivost in netoksičnost so lastnosti, zaradi katerih je polimer predmet intenzivnih raziskav. Njegova učinkovitost je bila potrjena tako za peroralno kot intravensko aplikacijo, medtem ko mehanizem privzema v tkiva še ni povsem razkrit.

Struktura in obnašanje GCPQ še nista v celoti pojasnjena in zahtevata dodatno pozornost, vendar pa njegova visoka molekulska masa omejuje uporabo običajnih spektroskopskih metod. Rešitev tega problema je depolimerizacija polimera z ustrezno metodo na fragmente, katerih velikost dopušča spektroskopsko analizo. Iskanju in optimizaciji ustrezne metode fragmentacije GCPQ in analizi rezultatov fragmentacije sem posvetila večji del magistrske naloge. Prav tako je del magistrske naloge namenjen sintezi polimerov z želenimi lastnostmi, ki so bili nato uporabljeni za pripravo in analizo nanodelcev v različnih topilih z namenom ovrednotenja vpliva lastnosti topila in polimera na velikost nanodelcev.

Ključne besede: hitosan, GCPQ, nanodelci, MALDI TOF, fragmentacija

List of abbreviation

Abbreviation	Meaning
% P	Degree of palmitoylation
% Q	Degree of quaternization
BBB	Blood brain barier
Da	Dalton
dGC	Degraded Glycol Chitosan
dGCPQ	Deuterated GCPQ
DLS	Dynamic light scattering
ESI	Electrospray ionization
GC	Glycol chitosan
GCPQ	Quaternary Ammonium Palmitoyl Glycol Chitosan
GIT	Gastrointestinal tract
GPC MALLS	Gel Permeation Chromatography Multi Angle Laser Light Scattering
kDa	kilo Dalton
M	Molar (mol/L)
MALDI TOF	Matrix Assisted Laser Desorption/Ionization Time- Of- Flight
Mn	The number average molecular weight
Mw	The weight average molecular weight
MWCO	Molecular weight cut-off
My	The viscosity average molecular weight
Mz	The size average molecular weight

nm	Nanometers
NMR	Nuclear Magnetic Resonance
PDI	Polydispersity index
PES	Polyethersulfone
PGC	Palmitoylated glycol chitosan
ppm	Parts per million
PTFE	Polytetrafluoroethylene
QUELS	Quasielastic light scattering
Rpm	Rounds per minute
TEM	Transmission electron microscopy
TFA	Trifluoroacetic acid

1. Introduction

Recent advances in chemical synthesis and recombinant DNA technology have enabled the development of immense quantities of biopharmaceuticals with great structural variety. With 95% of all drugs still being administered orally, the oral route of application is the most popular choice of drug delivery. The reasons behind this are acceptability, convenience, low costs and good patient compliance. The formulation of biopharmaceuticals, used for wide variety of diseases, among them also cancer and autoimmune diseases, is still challenging due to their poor permeation across biological barriers (such as gastrointestinal barrier and blood brain barrier), poor dissolution in GIT and poor stability in GIT. There are many different approaches to address this problem; creating nanoparticles using suitable polymer to encapsulate the drug, seems to be among the most successful ones. Nanoparticulate drug delivery systems improve bioavailability and biocompatibility of drugs and offer great potential in the drug delivery. With the use of nanoparticles, it is possible to increase drug solubility, achieve sustained drug release, diminish toxicity, increase enzymatic and physical stability of the drug, enhance drug transport across the intestinal mucosa and target drug delivery to a specific site in the organism. Chitosan based nanoparticles, such as GCPQ, are known to self-assemble in water, forming micelles and because of their biocompatibility, biodegradability and ability to improve drug transport across epithelial membranes, they have great potential as nanomedicines. Their efficacy has been confirmed for both oral and intravenous delivery route in drug delivery studies, whiles the mechanism by which they are taken into and interact with the tissues, is still being a subject of research. [1-7, 9, 10]

1.1 Chitin, chitosan and derivatives

Chitin and chitosan are natural amino-polysaccharides with great potential as a biomaterial with perspective in diverse expanse. Both polymers have unique structure and applications of a broad dimension in different industrial areas, including Biomedicine and Pharmacy. Their multidimensional properties, such as biocompatibility and biodegradability, environmental safety, antimicrobial activity and non-toxicity, are the reason for profound research and development of both polymers. [8-14]

Chitin is a structural polymer, a poly β-(1, 4) *N*-acetyl D-glucosamine, found in crustaceans, fungi, arthropods and yeast. Similar as the cellulose, this polysaccharide provides the

structural integrity and protection to organisms, plants and animals, where it is found. There are three different polymorphic forms of chitin occuring: α, β and γ. The degree of *N*-acetylation (the ratio of 2-acetamido-2-deoxy-D-glucopiranose to 2-amino-2-deoxy-D-glucopiranose) in chitin is typically 0.9 and it has an important effect on solubility and behaviour of chitin in solutions. [8]

Chitosan is a cationic polysaccharide, consisting of *N*-acetyl D-glucosamine and D-glucosamine residues, connected with β-(1, 4) glycosidic linkage, where the degree of *N*-deacetylation does not exceed 50%. Normally, it is obtained by deacetylation of chitin using different methods, for example deacetylation with 40% sodium hydroxide at 120°C for 1-3 h. Physical properties of chitosan are connected to variety of parameters, for example degree of deacetylation, molecular weight, the purity of the product and the sequence of amino and acetamido groups. [8-14]

The free amino group of chitin and chitosan enables modifications, leading to desired characteristics and biological functions (e.g. solubility). Apart from the amino groups, there are two hydroxyl groups, which can be modified using suitable chemical reactions, to improve solubility. Many different reactions, such as etherification, esterification, copolymerization, cross-linking, acetylation, quarternization, can take place, giving rise to a range of products with desired characteristics (biodegrability, biocompatibility, antibacterial activity, non-toxicity…). [8]

Chitin has drawn a lot of attention but due to its poor solubility, chitosan has been the centre of research lately. The aim is to develop chitosan derivatives with well-defined molecular structure and improved characteristics and functions. [8]

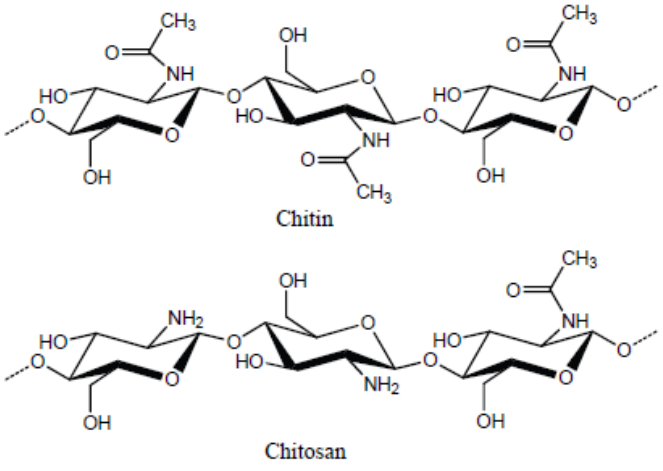

Figure 1: *Structures of Chitin and Chitosan [12]*

The development of water soluble chitosan derivatives also includes glycol chitosan. Glycol chitosan is soluble in water due to attachment of the hydrophilic glycol group on the free hydroxyl group, obtained in reaction between chitin and ethylene oxide, followed by deacetylation, resulting in O-acetylated glycol chitosan. Unaffected free amine group enables future modification without affecting favourable biological interactions. [11]

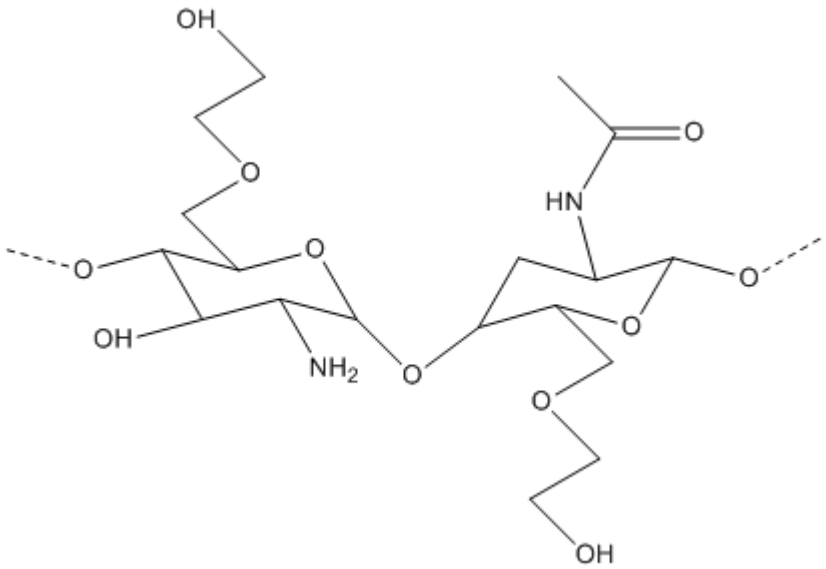

Figure 2: *Accepted structure of glycol chitosan*

1.2 Quaternary Ammonium Palmitoyl Glycol Chitosan

GCPQ (Quaternary Ammonium Palmitoyl Glycol Chitosan) is a derivative of glycol chitosan, obtained by covalent modification of the carbohydrate backbone with hydrophobic and hydrophilic groups to create an amphiphilic polymer (Mw < 20kDa-50kDa). These polymers self-assemble in aqueous media at low micromolar concentrations, creating 100 nm – 300 nm clusters of smaller, 10 – 30 nm large micellar aggregates. Soluble polymers with pendant amphiphilic or hydrophobic drugs are known as polysoaps and drug solubilising agents. [4, 15]

Hydrophobic drugs can be incorporated in the hydrophobic domains, formed at the centre of the micelles. Polymer properties can be tailored by varying the molecular weight of carbohydrate (typically 6kDa – 50kDa), the degree and nature of the lipidic derivatisation (typically 10-20% palmitoylation), and the degree and nature of the charged group (typically in the order of 10% quaternization). [15]

The polymer forms stable nanoparticles with molar polymer/hydrophobic drug ratios as high as 1:67 and improve the transfer of drug across biological barriers by 1 order of magnitude. GCPQ nanoparticles have shown great potential as a delivery system, which increases the transport of hydrophobic and also hydrophilic drugs across the GIT epithelium, cornea and brain-blood barrier. [1-7, 15]

High molecular weight (>500 Da), a high log P value (>5.0) and low gastrointestinal permeability are the main limitations when it comes to oral administration of a drug. GCPQ nanoparticles significantly enhance the oral absorption of hydrophobic drugs and to lesser extent the absorption of hydrophilic drugs. They increase the dissolution rate of hydrophobic molecules, by encapsulating high concentration of a drug inside stable nanoparticle. Next step is adhesion to and penetration into the mucus layer, thus enabling intimate contact between the drug and the gastrointestinal epithelium absorptive cells, prolonging residential time at the absorption site and enhancing the transcellular transport of hydrophobic compounds, without opening tight junctions. Recently, it has been discovered that GCPQ nanoparticles can successfully be used to facilitate oral absorption, prevent intestinal and plasma degradation and increase the uptake of neuropeptides, used for treating brain diseases, across blood brain barrier. [1-7]

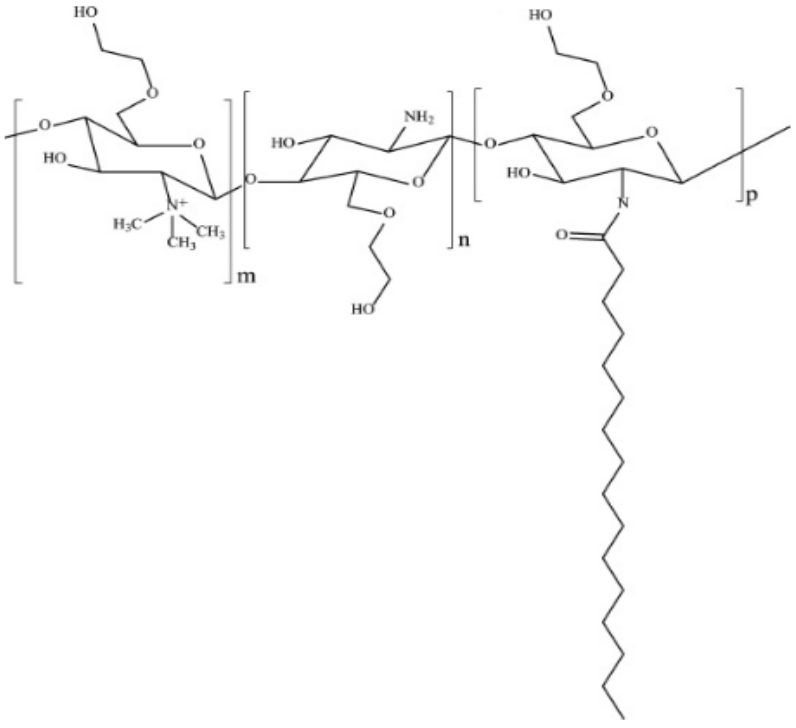

Figure 3: *Structure of Quaternary Ammonium Palmitoyl Glycol Chitosan [6]*

1.3 Fragmentation of chitosan based polymers

In order to allow structural analysis of the polymer, using different techniques, such as MALDI TOF and LC-MS/MS, a breakdown of the larger molecular weight material to fragments of suitable size is required.

Fragmentation methods, described in the literature, are typically being used on chitin, chitosan or other carbohydrates; none of the articles found was describing fragmentation of the GCPQ. Different fragmentation methods can roughly be organized in 3 groups:

- (inorganic) chemical fragmentation
- physical fragmentation
- enzymatic fragmentation

1.3.1 Chemical fragmentation

There are many different methods of chemical fragmentation for carbohydrates, as this type of fragmentation is very common. Different reagents can be used:

- $FeCl_3$ can be used as a catalyst, leading to more effective fragmentation, due to a molecule – ion interaction between $FeCl_3$ and the carbohydrates in aqueous solution. The $FeCl_3$ promotes the fragmentation already at low concentration. [16]

- Partially deacetylated chitin and chitosan can be successfully fragmented using H_2O_2 in low concentration. The fragmentation is random and the decrease in the average molecular weight of the polymer is believed to be of 1. order kinetics and is decreasing faster with increasing reaction temperature. The presence of transition metal ions in small quantities is crucial to cleavage of the β-(1, 4) glycosidic bond. Apart, for the fragmentation of the polymer to occur, it is necessary for the free amino groups to be present in certain amount. Experimental conditions, such as temperature, physico-chemical characteristics of the polymer and the concentration of the reagent H_2O_2, have an important impact on the fragmentation of the polymer and formation of the smaller fragments. The fragmentation rate is much faster compared to ultrasonic fragmentation and it is comparable to the rate of the enzymatic hydrolysis of chitosan. [17]

- Fragmentation using acids – one of the oldest and the most common methods of the carbohydrate fragmentation. Partial hydrolysis of chitin and chitosan to obtain different derivatives using different acids is very popular. A high variety of acids has been in use, such as hydrochloric acid, sulphuric acid, phosphoric acid and of course nitrous acid. [17]

1.3.2 Physical fragmentation

- Thermal fragmentation (pyrolysis) – it can lead to the formation of many different volatile and non-volatile products. Different carbohydrates demand different temperatures to undergo thermal decomposition, with the temperature of only 100°C needed for cellulose. With increasing temperature, the concentration and number of volatile products increases. [18]
- Ultrasonic fragmentation – the fragmentation rate is much slower compared to chemical fragmentation. [17]

1.3.3 Enzymatic fragmentation

Fragmentation of carbohydrates can also be achieved using many different enzymes, which can cleave the β-(1, 4) glycosidic bond.

- Mixture of cellulase, alpha amylase and proteinase can depolymerize chitosan to obtain smaller oligocsaccharides. It can also be fragmented by chitinases, chitosanases and lysozimes, as well as with unspecific enzymes such as cellulase, lipase and bromelain. [19]
- Lysozyme is one of the most important enzymes for fragmentation of chitin and chitosan. Different lysozymes can be used; most common are human and hen egg white lysozymes. The fragmentation rate can be controlled by the ratio of acetylated and deacetylated units and it increases strongly with increasing fraction of N-acetylated units for both enzymes. [20]

Chemical fragmentation of GCPQ, using nitrous acid, has many advantages compared to other methods- it has already been used previously in our laboratory for fragmentation of GCPQ, so it was already studied and well known. It is known that modifications such as acetylation, palmitoylation and quaternization should remain intact, which is of great

importance when trying to see the distribution of those substituents on the polymer backbone. Also the kinetics of the reaction is well known, the number of glycosidic bonds breaking is stoichiometric to the amount of nitrous acid used, what makes it possible to control degree of depolymerisation. Enzymatic methods are specific and more controllable but the high cost and lesser availability of chitosanases are the reasons for limited use. [19] The problem of enzymatic reaction is also reproducibility. It is easier to work with acid instead of enzymes, which are very sensitive and demand mild reaction and storage conditions. The fragmentation of GCPQ with lysozyme has already been tested in our laboratory and the results showed no fragmentation.

1.4 Fragmentation of GCPQ with nitrous acid

The number of cleaved glycosidic bonds can be considered stoichiometric to the quantity of nitrous acid used. The cleavage of the bond involves deamination of a D- unit and formation of 2, 5-anhydro-D-mannose at the new reducing end. The newly formed reducing end is not stable, so the common procedure is reduction with $NaBH_4$ to obtain 2, 5-anhydro-D-mannitol. [14]

The fragmentation of glycol chitosan with nitrous acid was adapted, from a previously published procedure [11], which is illustrated below.

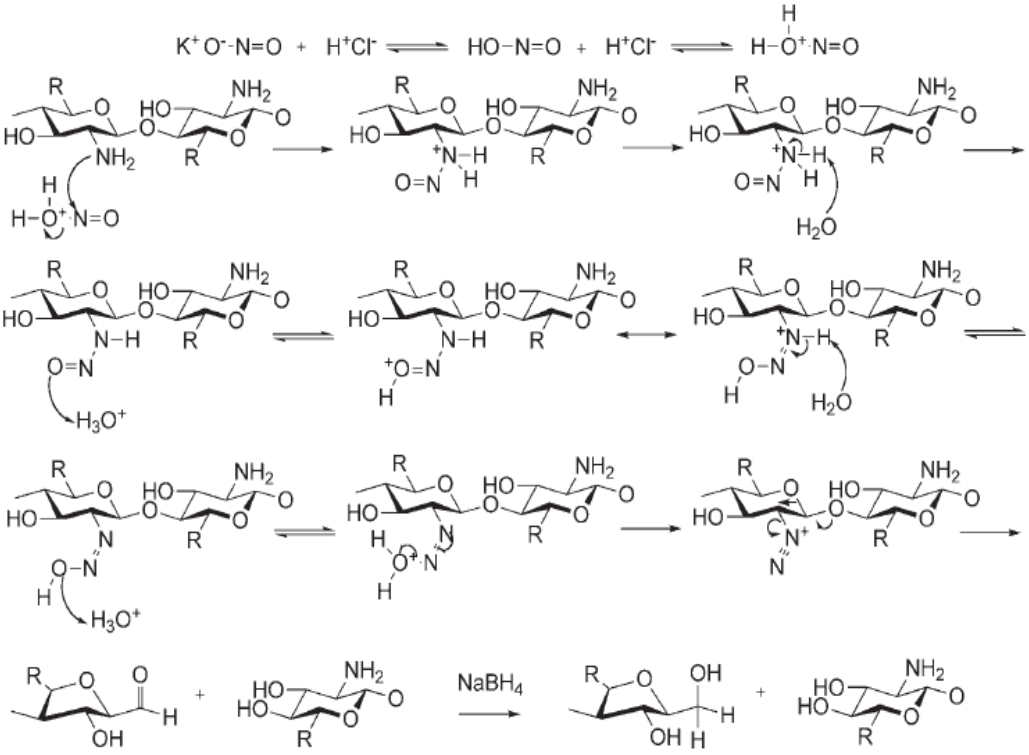

Figure 4: *Fragmentation of GC via diazotization of the primary amine with nitrous acid [11]*

Nitrous acid in water forms a variety of nitrosating agents, regarding the pH. The strength of these nitrosating agents differs and it has an impact on the size of the fragments obtained. In our study, the pH=5.1 was used, at which the nitrosating agent may be nitrosyl chloride or possibly nitrous anhydride. These nitrosating species are not as agressive, leading to a higher molecular weight of the polymer fragments. [11]

The reaction with nitrous acid offers many advantages- it is selective, fast (also in mildly acidic solutions and at room temperature) and easily controlled, also the stoichiometry and reaction products are well established and known. Glycosidic bond gets cleaved due to selective reaction of nitrosating species, originating from nitrous acid with free amino groups. The reactions kinetics is of the first order with respect to nitrous acid and remains constant also after the reduction of Mw of chitosan, confirming the depolymerisation kinetics are non-dependent of the size of the chitosan substrate. Overall rate of depolymerisation is proportional to the concentration of free amine groups. Rate limiting step is the nitrosation of unoprotonated amine by the nitrous acidium ion. With increase of degree of deacetylation of chitosan the nitrosation rate decreases, due to the reduction in nucleophilicity of the amine groups. [21, 22]

Glycosidic bonds should break next to an unmodified amino group, next to deacetylated units. The percent of modifications on GCPQ is usually around 45% (palmitoylation + quaternization + acetylation), which means that the biggest fragment obtained could be 45% of the molecular weight of the whole GCPQ molecule (if all the modification would occur one after another on the sugar backbone of the GCPQ). The smallest fragment that could be formed would be a monomer.

Different products of the depolymerisation are possible (A= acetylated, P= palmitoylated, Q= quaternized unit, D= deacetylated unit). There could be 3 or more units between 2 deacetylated units, which would result in formation of tetramers (similar with 4 or more units between 2 deacetylated units).

Different side reactions could occur during the fragmentation process. Under pH=3, nitrosation of amide groups on acetylated unit could occur, which would lead to the formation of N–nitrosamide. This product is unstable at physiologic pH and decomposes to a diazohydroxyl, followed by a diazonium cation and results in the cleavage of the glycosidic bond. This process can be followed by monitoring the degree of acetylation before and after

the fragmentation. If no change in degree of acetylation is observed, it is possible to conclude conversion of amide groups to N–nitrosamides did not occur. [11]

Nitrosation of tertiary amines, resulting in formation of N–nitrosamines due to the cleavage of a glycol group could happen. However, this process is significant at higher temperatures, which have not been used in our experiment. [11]

Nitrosation of secondary amine could occur, but the fragmentation at higher pH inhibites the formation of N–nitrosamines. Also no direct nitrosation should occur between quaternary ammonium compound and nitrite in acidic solutions even at higher temperatures. [11]

1.5 Methods of characterization

Different methods of characterization, described below, were used to determine the characteristics of synthesized polymers and nanoparticles and to analyse the fragmentation process of the polymer.

1.5.1 Gel Permeation Chromatography Multi Angle Laser Light Scattering (GPC MALLS)

Gel permeation chromatography is a type of size exclusion chromatography, which separates analytes based on size differences. It can be used as a separation or purification technique. Different polymer characteristics can be determined and obtained using gel permeation chromatography, such as different molecular weights including the number average molecular weight (M_n), the weight average molecular weight (M_w), the size average molecular weight (M_z), or the viscosity average molecular weight (M_v). With GPC, it is also possible to determine the polydispersity index (PDI) of a polymer batch. PDI indicates the molecular mass distribution in a polymer sample. Its value can be 1 or greater, with the value approaching 1 as polymer chains lengths approach uniform. [23]

Analyte molecules are separated based on differences in their hydrodynamic volume. Smaller molecules enter the pores of the column packing easily and remain inside the pores longer, extending their retention time. Bigger molecules, on the other hand, have difficulties entering the pores, spend less time inside the pores and elute faster. If the analyte is too big according to the pores, it will not retain at all, which means it will elute without entering the pores. On the contrary, molecules much smaller than the pores, will retain completely. Each column has a certain limited size range of molecular weight that can be separated with it. Appropriate

column packing should be chosen for analysis of specific analyte, regarding its size and chemical characteristics. [23]

Gel permeation chromatography can be used connected to Multi angle laser light scattering detector, which is molecular weight sensitive detector and to RI detector, which is concentration sensitive detector. First, analyte molecules are separated based on size with gel permeation chromatography and then they pass on to the MALLS detector, where they are irradiated by the laser light. There are 18 detectors placed on different angles measuring light scattering. Based on the quantity of the scattered light, the molecules size is calculated. Then dn/dc value for the sample has to be determined, using 6 different concentrations of the sample solution. Dn/dc is a correction factor, which gives the change of refractive index with increasing concentration of the sample. Based on this value, molecular weight of the analyte is calculated. [23]

Gel permeation chromatography MALLS was used to get the first indication of the fragmentation process with nitrous acid. Smaller fragments that would form in the process of fragmentation would cause the shift in the laser light scattering, what would be seen on the chromatogram as the presence of different peaks, indicating that the fragmentation is happening. But the problem is the size of fragments: GPC can only detect fragments, bigger than 1kDa, which means that if any smaller fragments form during the fragmentation, they cannot be detected using GPC. That is the reason why other techniques, such as MALDI TOF, were used. [23]

1.5.2 Mass spectrometry

Mass spectrometric analysis is carried out in the gas phase on ionized analytes. A mass spectrometer consist of an ion source, that produces ions of an analyte, a mass analyser that measures the mass-to-charge ratio (m/z) of the ionized analytes and a detector, that detects the quantity and abundance of analyte ions for each m/z ratio. Electrospray ionization (ESI) and Matrix-assisted laser desorption/ionization (MALDI) are the two techniques, most commonly used to volatize and ionize the proteins, peptides or other large and sensitive species for mass spectrometric analysis. ESI ionizes the analytes directly out of a solution, while MALDI sublimates and ionizes the sample out of a dry, crystalline matrix using laser pulses. ESI can be conveniently coupled to different liquid based separation methods (e.g. chromatographic and electrophoretic), without a need to previously remove the solvent. [24]

1.5.2.1 Matrix Assisted Laser Desorption/ Ionisation Time- of- Flight (MALDI TOF)

Matrix-Assisted laser desorption/ionization is a solid state ion source, often used in mass spectroscopy. It enables the formation of intact gas phase ions from a variety of big, non-volatile and thermally sensitive species such as proteins, peptides, oligonucleotides, synthetic polymers and large inorganic compounds. It does not require extended sample preparation and it has a large tolerance towards different contaminants, which are common in chemistry, for example buffers, salts and detergents. [25]

MALDI is a two phase process. The first step is preparation of a solid solution deposit of analyte- doped matrix crystals, in which analyte molecules are embedded through the matrix and completely separated from one another. For a compound to be suitable as matrix, it needs to have a strong absorption at the laser wavelength. In the second step, the solid solution is irradiated by short pulses of laser light over a short duration. This causes rapid heating and sublimation of the matrix crystals and its expansion into the gas phase, converting intact analyte in the expanding matrix plume. [24, 25]

Time-of-flight is a type of mass analyser used in mass spectroscopy. The analyte ions are accelerated by an electric field applied. Once they enter a flight tube, there is no electric field and the analyte ions are shifted differently due to their different velocities, which reflect their m/z ratio. Mass to charge ratios are determined by measuring the time that ions take to travel through a field-free region of the flight tube between the source and the detector. The instrument has high sensitivity and no upper mass limit (300 kDa and more). There are many types of TOF instruments, such as linear TOF and reflectron TOF instrument. MALDI TOF is widespread and powerful tool for mass spectroscopy due its great accuracy, simplicity, high resolution and sensitivity. [24, 25]

1.6 Formation and characterization of GCPQ nanoparticles

When in solution, GCPQ is known to self-assemble, forming nanoparticles. The conditions (pH, ionic strength…) of the solvent and characteristics of polymer (%P, Mw…) affect the formation and size of the particles. My aim was to compare the size of particles of three GCPQs with different characteristics in different solvents. This way it would be possible to predict how polymer and solvents' characteristics affect particles size.

1.6.1 Nanoparticles characterization methods

For determining the average particles size, DLS was used. TEM enables the visualization of the particles' morphology and also gives the size of a specific particle that we choose.

1.6.2.1 Transmission Electron Microscopy (TEM)

TEM is used to display images of a thin specimen, to visualise the morphology of the sample. It offers a magnification range from 10^3 to 10^6. The instrument can be divided in three sections:

The illumination system consists of the electron gun with at least two condenser lenses. The lenses focus beam of the electrons onto a thin specimen. This part of the microscope is used to determine the diameter of the electron beam at the specimen and the level of intensity in the final image. The electron gun consists of an electron source, usually referred to as a cathode (due to its high negative potential) and an electron-accelerating chamber. There are many different types of electron source, based on different principles. [27]

The specimen stage is a part of microscope which holds specimens stationary and also enables the intentional movement of the specimen if desired. The spatial resolution of the final TEM image depends on the mechanical stability of the specimen and therefore this part of the microscope is very important. [27]

The imaging system produces magnified image of the specimen, using three or more lenses. The image can be displayed on a fluorescent screen, on photographic film or on the monitor screen of an electronic camera system. [27]

TEM microscope and the light microscope both operate on the same basic principles- the main difference is that the TEM uses electrons as a source of light. Therefore, the much lower wavelength of electron enables a thousand times better resolution compared to a light

microscope. Electromagnetic lenses focus electrons into a very thin beam, which then travels through the analyte. Based on density of analysed material some electrons are scattered from the beam, while others reach the fluorescent screen at the bottom of the microscope. This results in formation of a "shadow image" of the analyte. Regarding the density of different parts of the sample, different intensity of darkness is displayed on the image. The image can be captured with a camera for additional studies or it can be studied directly.

1.6.2.2 Dynamic light scattering (DLS)

Dynamic light scattering (DLS) is a light scattering technique, which enables determining the size and size distribution of small particles and molecules, smaller than 1000 Da. It is a non-destructive and well-established technique, which can measure particles of a size below 10 nm. One of advantages is also small sample volume, required for analysis (depends also on the size of the cuvette). The principles of dynamic light scattering are based on the Brownian motion of suspended particles or molecules. The particles will therefore scatter laser light at different intensities, based on their size - bigger particles scatter more light compared to the smaller ones. The velocity of the Brownian motion is obtained with analysis of these light intensity fluctuations. Using the Stokes-Einstein relationship, the average particles size is measured. The main drawback of the DLS is its sensitivity to all kind of contaminant's particles present (dust, fibers…) which affect the accuracy of results. [28, 29, 30, 31]

The primary and most stable parameter is given as the Z-Average size or Z-Average mean, also known as the cumulants mean. Intensity distribution of particle sizes is fundamental size distribution, obtained from a DLS analysis. It is naturally weighted regarding the intensity of light scattering, caused by each particle fraction. The particle scattering intensity of polymers is proportional to the square of the molecular weight. The problem of the intensity distribution is a presence of small aggregates or agglomerates or large particle populations, which can affect and dominate the distribution. Using Mie theory, it is possible to convert intensity distribution to a volume distribution or a distribution by number. However, these two distributions are only useful for comparative purpose and are not absolute. [28, 29, 30, 31]

2. Aims and objectives

Aims and objectives of this master thesis can roughly be organised in two sections:

2.1 Synthesis and characterization of GCPQ

- Synthesis and characterization of three polymer batches with desired characteristics, following the synthesis guidelines
- Preparation of the polymer nanoparticles, using synthesized polymer batches and different solvents
- Characterization of the formed nanoparticles with DLS to obtain the average size of the particles and TEM to visualize the morphology of the particles
- Establishment of the relationship between polymer's and solvents' characteristics on the average size of the nanoparticles

2.2 Fragmentation of GCPQ

- Finding and applying a method of fragmentation, suitable for GCPQ
- Analysis and optimization of the chosen fragmentation method, using different analytical methods (GPC MALLS, MALDI TOF), to obtain fragments of desired size (< 1000 Da)
- Analysis and interpretation of the MALDI TOF results in order to obtain information regarding the polymer's structure and a better insight into the fragmentation process

3. Materials, instruments and methods

3.1 Materials

In the experimental section, different materials, including reagents, solvents, filters and gasses were used. Most of the material used was purchased from Fischer Scientifics UK Ltd, Sigma Aldrich Chemical Co. and Cambridge Isotope Laboratories Inc, unless otherwise stated.

Reagents: Glycol Chitosan, Sodium hydroxide, Palmitic acid *N*-hydroxysuccinimide ester, Sodium bicarbonate, Sodium iodide, Methyl iodide, *N*-methyl-2-pyrrolidone, Anhydrous Sodium acetate, Sodium Chloride, Glacial acetic acid, Potassium dihydrogen phosphate, Potassium nitrite, Sodium borohydride, 1% w/v uranyl acetate aqueous solution, Trifluoroacetic acid, Sinapinic acid

Materials: Amberlite IRA-96 Resine, PES Filters 0.22 µm, PTFE Filters 0.45 µm, Dialysis Tubing (3.5 kDa, 7 kDa, 12-14 kDa)

Solvents: Deionized water, Milli-pore double deionized water (<18Ω), Methanol-D4, Deuterated water, Methanol HPLC gradient, Absolute Ethanol, Hydrochloric Acid 32-38% solution, Diethyl Ether, Acetonitrile

Gasses: Nitrogen

3.2 Instruments

- Sonicator, Qsonica, LLC,
- GPC-MALLS equipped with: Dawn Heleos II MALLS detector (120mW solid-state laser operating at λ = 658 nm), Optilab rEX interferometric refractometer (flow cell: 7.4 uL, λ = 658 nm), quasielastic light scattering (QELS) detectors (Wyatt Technology Corporation, Santa Barbara, CA, USA), and Agilent 1200 autosampler (Agilent Technologies, UK)
- Applied Biosystems Voyager- DE Pro Biospectrometry workstation (MALDI TOF)
- Zetasizer Nano S90, Malvern, UK
- Transmission Electron Microscopy (TEM), Philips CM 120, Biotwin
- NMR, Bruker Avance 400 MHz NMR spectrometer, equipped with broadband and selective (^{1}H and ^{13}C) inverse probes

4. Experimental part

4.1 Synthesis and characterization of GCPQ

4.1.1 Synthesis of GCPQ

Three batches of Quaternary Ammonium Palmitoyl Glycol Chitosan (GCPQ) with desired characteristics were synthesized, following the procedure and guidelines, described below.

4.1.1.1 Degradation of glycol chitosan

Certain amount of glycol chitosan (with degree of acetylation above 5%, detected using ^{1}H-NMR) was suspended in 4M hydrochloric acid at the room temperature to obtain concentration of 1.3% w/v (1g of GC in 76 ml of 4M HCl). The starting amount of GC depends of the amount of GCPQ, desired to yield. 4M hydrochloric acid was prepared by diluting 10M hydrochloric acid with deionized water. The solution was then shaken at 125 rpm for predetermined time, in a water bath, at the constant temperature of 50°C (degradation time of GC depends of the desired molecular weight of GCPQ, as shown in *Table I*).

Table I*: Guidelines for degradation of glycol chitosan*

dGC Molecular weight after degradation (Da)	GC degradation time (hours)
80000 – 120000	0 (undegraded GC)
35000 – 45000	2 (GC2)
10500 – 12000	24 (GC24)
6500 – 8500	48 (GC48)
2800 – 4000	9 hour redegradation of GC48

Next, the temperature of the solution was reduced in order to stop the reaction of degradation, by placing the flask with the solution into the fridge for few minutes. After cooling to the room temperature, the solution was exhaustively dialyzed against deionized water (5 L of deionized water with six changes of deionized water over 24 hours, at least 1-2 hours between two changes) by transferring the solution into seamless cellulose dialysis tubing with a molecular weight cut-off of 3500 Da. The dialysate was subsequently freeze-dried at -20°C,

and the product was recovered as a beige cotton-wool-like solid.

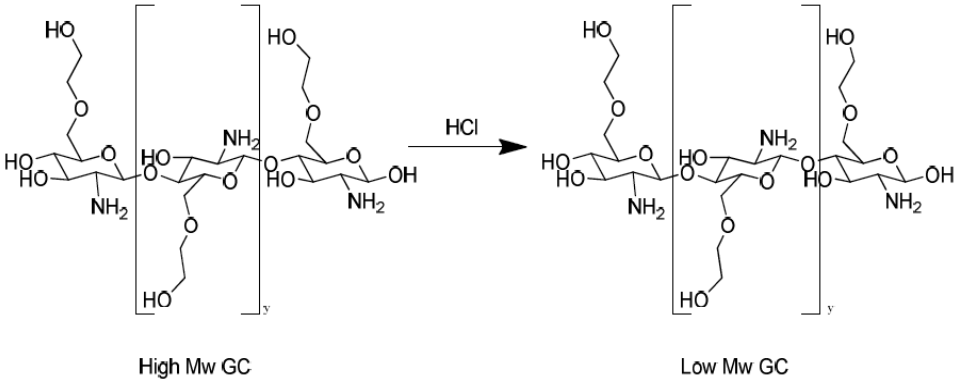

Figure 5: *Reaction of acid degradation of glycol chitosan in 4M HCl (y of the low Mw GC is smaller than the y of high Mw GC)*

4.1.1.2 Palmitoylation of degraded glycol chitosan

Degraded glycol chitosan (dGC) and sodium bicarbonate (376 mg per 500 mg of dGC) were dissolved in the mixture of double deionized water and absolute ethanol to give 0.5% w/v dGC solution (500 mg of dGC in the mixture of 24 ml of absolute ethanol and 76 ml of double deionized water). Separately, the solution of Palmitic acid *N*-hydroxysuccinimide ester in absolute ethanol (792 mg of PNS in 150 ml of absolute ethanol per 500 mg of dGC) was prepared and added drop-wise to the solution of dGC, while stirring on the magnetic stirrer, using a separating funnel (protected from light with aluminium foil). Subsequently, the solution was stirred on the magnetic stirrer, protected from light, for another 72 hours, at the room temperature.

After 72 hours, ethanol was removed from solution by rotary evaporation at 50-52°C and under reduced pressure. The remaining aqueous phase was extracted using diethyl ether to remove any ethanol remaining with slow, swirling movements. Phases were separated to obtain clear top organic phase, bottom aqueous phase and a fatty layer in between which represents palmitoylated chains of the glycol chitosan. Fatty layer phase was collected together with aqueous phase. The extraction was repeated twice.

The solution (extracted water phases and fatty layer) was exhaustively dialyzed against deionized water (5 L of deionized water with six changes of deionized water over 24 hours, at least 1-2 hours between two changes) by transferring the solution into seamless cellulose

dialysis tubing with a molecular weight cut-off of 12000-14000 Da. After dialysis, solution was transferred into freeze drying bottles and freeze-dried at -20°C to obtain beige cotton-wool like solid.

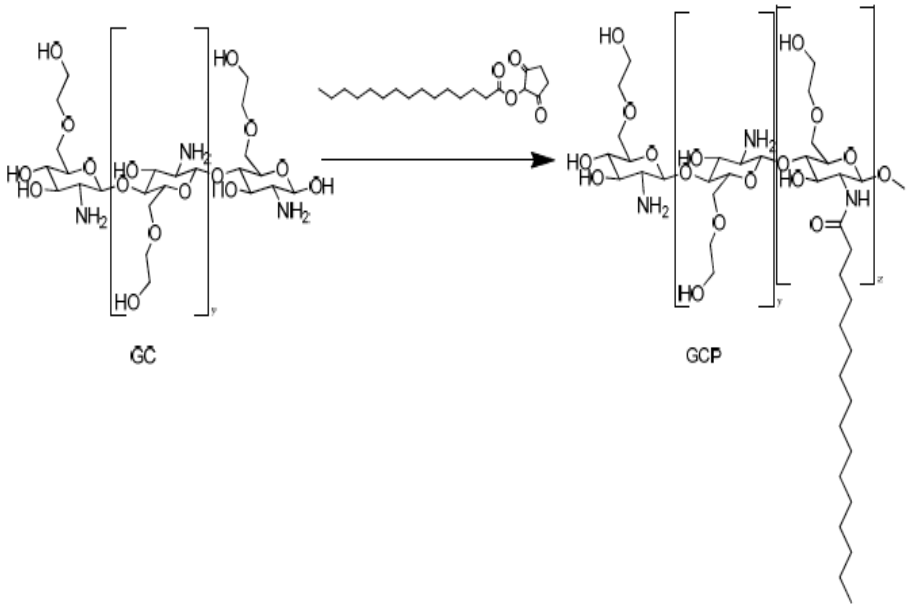

Figure 6*: Palmitoylation of degraded glycol chitosan*

4.1.1.3 Quaternization of palmitoylated glycol chitosan

Palmitoylated glycol chitosan (PGC) was weighted and dispersed in *N*-methyl–2 pyrrolidone to obtain concentration of PGC 1.2% w/v (300 mg of PGC in 25 ml of *N*-methyl-2 pyrrolidone). The dispersion was stirred vigorously for 3-16 hours, until a foamy dispersion was obtained. In the meantime, oil bath was preheated to 36°C in order to reach stable temperature throughout the reaction (the temperature should not exceed 38°C). Solution of NaOH in absolute ethanol (40 mg of NaOH for 300 mg of PGC, in 4 ml of absolute ethanol), sodium iodide (45 mg for 300 mg of PGC) and methyl iodide (0.44 ml for 300 mg of PGC) were added to the PGC solution. The final solution was being stirred in a preheated oil bath under nitrogen atmosphere (obtained by filling a balloon with nitrogen gas and clamping it closed until it is attached to the flask, then releasing the clamp) for 3 hours.

After 3 hours, the product was precipitated in diethyl ether and left overnight. Next day, stable yellow hygroscopic precipitate was washed with diethyl ether and dissolved in deionized water (100 ml of deionized water for 400 mg of PGC) to give a pale yellow dispersion, which was dialysed exhaustively against deionized water (5 L of deionized water with six changes of deionized water over 24 hours, at least 1-2 hours between two changes) by transferring the solution into a seamless cellulose dialysis tubing with a molecular weight cut-off of 7000 Da. After dialysis, the content of membranes was drained into a beaker and instead of freeze drying, iodide was removed first.

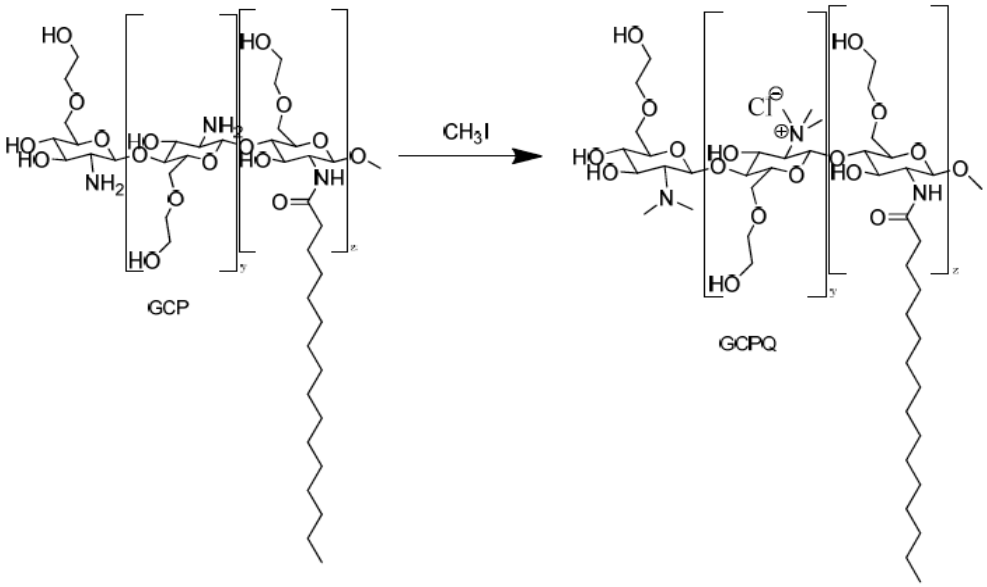

Figure 7*: Quaternization of palmitoylated glycol chitosan*

4.1.1.4 Removal of iodide

The column was prepared by packing a small piece of glass wool in the neck of the separating funnel and adding dry Amberlite IRA-96 (aprox. 100 ml). The resin was then washed with 150 ml of HCl, followed by 8 L of deionized water (the pH of the column after washing should be neutral). The funnel was left wet, with tap closed, overnight. Next day, the column was washed with further 2 L of deionized water. The dialysate was slowly passed through the column and collected directly into freeze drying bottles. The column was subsequently washed with deionized water. The solution was freeze- dried at -20°C to obtain white, yellowish or brownish cotton- like solid.

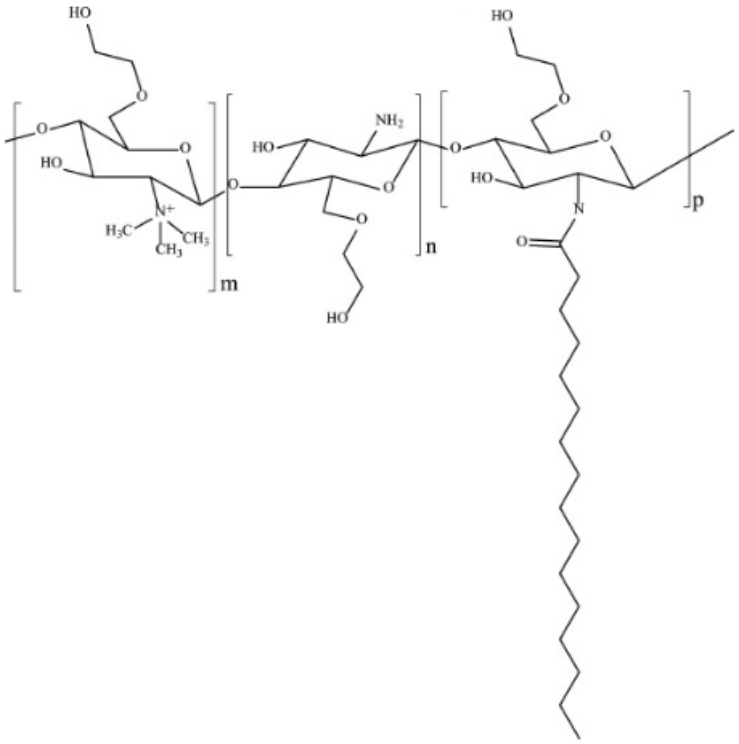

Figure 8*: Structure of Quaternary Ammonium Palmitoylated Glycol Chitosan*

4.1.2 Characterization of GC and GCPQ

Synthesized batches of polymer were characterized, using different methods, to determine the degree of palmitoylation, the degree of quaternization, the molecular weight and the polydispersity index.

4.1.2.1 GPC MALLS

The Gel permeation chromatography Multi Angle Laser Light Scattering was used to determine the molecular weight (Mw and Mn) and the polydispersity index of glycol chitosan, used for synthesis of GCPQ and of synthesized GCPQs.

Measurements were performed using a DAWN EOS MALLS detector (λ=690nm), Optilab DSP interferometric refractometer (λ=690nm) and a quasielastic light scattering (QELS) detector. The column system used was a POLYSEP-GFC-P guard column (35x7.8 mm, Phenomenex, Macclesfield, U.K.), attached to a POLYSEP-GFC-P 4000 column (300x7.8 mm, Phenomenex).

Measurements were performed at room temperature with a mobile phase flow rate of 0.7 ml/min to prevent high pressure on the column. After analysis, data was processed using ASTRA for Windows version 5.3.4 software (Wyatt Technology Corporation).

Prior analysis, samples were prepared by dissolving GCPQ or GC in the mobile phase, to obtain the concentration of 5 mg/ml. Before injection, samples were filtered through 0.22 µm PES filters to remove bigger particles.

Specific refractive index increments (*dn/dc*) of GCPQ were measured in the same mobile phase as used for analysis, with an Optilab DSP interferometric refractometer (λ=690nm). 6 samples with the concentration range of GCPQ 0.1 to 0.6 mg/ml were prepared and filtered using 0.22 µm PES filters. Prepared samples were manually injected in increasing concentration, starting with a blank injection (mobile phase). Flow rate of mobile phase used was 0.3 ml/min. After analysis, data was processed using ASTRA for Windows version 5.3.4 software (Wyatt Technology Corporation). The refractive index obtained was used to calculate molecular weight of the synthesized polymer.

Different mobile phases were used for GC and GCPQ analysis. When analysing GC, mobile phase used was 500 mM acetate buffer (0.3 M anhydrous sodium acetate, 0.2 M glacial acetic acid, pH = 4.5). For GCPQ analysis, the mobile phase used was a mixture of 500 mM acetate buffer (0.3 M anhydrous sodium acetate, 0.2 M glacial acetic acid, pH = 4.5) and methanol (35:65 v/v).

4.1.2.2 ^{1}H-NMR

NMR analysis was carried out in order to confirm the identity of the polymer and to calculate the degree of palmitoylation and quaternization of the polymer. GCPQ was dissolved in deuterated methanol (CD_3OD) to give the concentration of 1% w/v, while GC was dissolved in deuterated water (D_2O). The level of palmitoylation was calculated by comparing the ratio of palmitoyl methyl protons to sugar unit protons (Equation *1*) and the level of quaternization was calculated by comparing the ratio of quaternary ammonium methyl protons to sugar unit protons (Equation *2*). Anomeric proton was not acknowledged in the calculation because the high molecular weight of the polymer usually prevents us to see the anomeric proton signal clearly on the ^{1}H-NMR spectrum. The protons acknowledged were the protons of the C3-C8, 9 of them altogether, which is accurate enough for calculation of polymers' characteristics.

4.1.2.2.1 ^{1}H-NMR of GCPQ

Five main signals should be displayed on the ^{1}H-NMR spectrum of GCPQ:

- The area between 0.85-0.9 ppm represents the triplet of the palmitic acid chain end
- The peak around 1.2 ppm represents the palmitic acid chain
- 2.2-2.4 ppm peak represents the signal of the CH_2 of the palmitic acid chain close to the C=O
- The area under the peak around 3.3 ppm represents the quaternized group
- The area under the peak between 3.5-4 ppm represents the sugar backbone
- The peak at 4.8 ppm is attributed to the solvent, deuterated methanol

After integrating all these signals to obtain the area value under each peak, the degree of palmitoylation and of quaternization are calculated using following formulas:

Equation *1:*

$$\% \text{ of Palmitoylation} = \frac{\text{area of the CH3 signal / number of hydrogens CH3}}{\text{Area of sugar chain / number of hydrogens of the sugar chain}}$$

Equation *2:*

$$\% \text{ of Quaternization} = \frac{\text{area of the N(CH3)3 signal / number of hydrogens N(CH3)3}}{\text{Area of sugar chain / number of hydrogens of the sugar chain}}$$

4.2 Formation and characterization of GCPQ nanoparticles

4.2.1 Nanoparticles formation

Polymer particles were formed by dissolving synthesized polymers in different solvents to obtain 5 mg/ml concentration and then by sonicating samples using probe sonicator at the suitable amplitude.

All the solvents used were filtered before use with 0.45 µm PTFE filters. Following solvents were used:

- double deionized water
- Phosphate buffer
- Simmulated gastric fluid- SGF (without pancreatine)

SGF was prepared following the procedure, described in European Pharmacopoeia. [26]

Briefly, NaCl was dissolved in the mixture of 1M HCl and double deionized water to give the pH of 1.2. Non- enzymatic SGF was used to avoid possible degradation of polymer, caused by the enzymes.

Phosphate buffer was prepared following the procedure, described in the European Pharmacopoeia. [26] Briefly, 0.2M NaOH and 0.2M KH_2PO_4 were dissolved in double deionized water, to give the pH of 6.8.

During the sonication, the samples were kept on ice to prevent heating. Sonication was carried out for two intervals of 5 minutes for each sample, with 2 minutes of break in between intervals. The amplitude of sonication was adjusted to each sample.

After sonication, samples were degassed using automatic degasser for 5 minutes, to remove bubbles. If there were still bubbles present after first 5 minutes, samples were degassed for another 5 minutes.

Before analysis, samples were filtered again with 0.45 µm PTFE filters. Sonicated, degassed and filtered samples were then transferred into an Eppendorf tube (1.5 ml) and analysed immediately with DLS and TEM.

4.2.2 Nanoparticles characterization

Polymer nanoparticles were characterized to determine the average particles size in different solvents. Additionally, TEM images of different polymer batches in different solvents were taken to visualise the morphology of the particles.

4.2.2.1 TEM

The samples were prepared fresh before analysis, using previously described procedure (*Chapter 4.2.1*). A drop of the sample was applied to the copper slit and the drop of the contrasting reagent (1% w/v uranyl acetate aqueous solution) was added. Negative staining technique was used.

4.2.2.2 DLS

The samples were prepared fresh before analysis, using previously described procedure (*Chapter 4.2.1*). The polystyrene 40 µL cuvettes were used to perform measurements. All experiments were performed in three batches. The zeta average of particles was determined in different solvents for different polymer batches.

4.3 Fragmentation of GCPQ

4.3.1 Fragmentation of GCPQ with nitrous acid

The fragmentation of GCPQ with nitrous acid was adapted from the procedure, proposed by Knight *et al* [11]. Briefly, certain amount of GCPQ was dissolved in double deionized water to give the concentration of 0.1% m/w. Under magnetic stirring, 1M hydrochloric acid or 1M NaOH was added to obtain the pH of 5.1. Next, solution was bubbled with N_2, 1M KNO_2 was added and the reaction mixture was left stirring. At predetermined times, sodium borohydride in suitable amount was added and allowed to react for additional 30 min, to reduce the terminal aldehyde groups to hydroxyl groups, while on ice. After 30 minutes, samples were stored in the freezer until analysis.

Table II*: Reactants and quantities used in reaction of fragmentation*

Reactant	Mw (Da)	Quantity
GCPQ		40 mg
H_2O	18	3.68 ml
KNO_2	85.10	0.067 ml
$NaBH_4$	37.83	7.56 mg

Fragmentation was done using two polymers with different characteristics, described below (*Table III).* Both polymers had a similar molecular weight, but one of them had a high degree of palmitoylation and quaternization, while the other one had a low degree of palmitoylation and quaternization. The degree of substitution of these two polymers is different, so the reaction of fragmentation should result in formation of different size of fragments.

Table III*: Characteristics of polymer batches, used for fragmentation reaction*

POLYMER BATCH	Mw (Da)	PDI	%P	%Q
GCPQ B3E	21000	4.9	34.6	14.6
GCPQ Q23	23000	2.3	4.0	3.0

The reaction was sampled at predetermined time points and analysed with MALDI TOF, to evaluate the reaction kinetics: after 1 hour, after 6 hours, after 24 hours and after 48 hours of fragmentation.

4.3.2 Optimization of fragmentation reaction

4.3.2.1 GPC MALLS

The GPC MALLS was used to observe the change in the molecular weight of the polymer, due to fragmentation. If fragmentation of the polymer occurred, smaller fragments would form, which would be seen as the shift of the polymer peak to the right - the retention time of smaller fragments is longer compared to bigger fragments. Undegraded GCPQ was used as a standard solution.

Measurements were performed using a DAWN EOS MALLS detector (λ=690nm), Optilab DSP interferometric refractometer (λ=690nm) and a quasielastic light scattering (QELS) detector. The column system used was a POLYSEPGFC-P guard column (35x7.8 mm, Phenomenex, Macclesfield, U.K.) attached to a POLYSEP-GFC-P 4000 column (300x7.8 mm, Phenomenex).

Measurements were performed at room temperature with a mobile phase flow rate of 0.6 ml/min to prevent high pressure on the column. After analysis, data was processed using ASTRA for Windows version 5.3.4 software (Wyatt Technology Corporation). The mobile phase used was a mixture of methanol and acetate buffer (500mM), 65/35.

Table IV*: Characteristics of the polymer used*

POLYMER BATCH	Mw (Da)	%P	%Q
GCPQ 7AI	19000	10	6.5

The reaction was carried out following the procedure, described previously (*Chapter 4.3.1*) and sampled at predetermined time points: after 1 hour, after 2 hours, after 6 hours and after 8 hours of fragmentation.

4.3.2.2 Mass spectroscopy

Prior analysis, samples were purified to remove salts and impurities, originating from fragmentation reaction and polymer synthesis, which could affect sensitivity of the method and results. Briefly, reusable single sample fast micro equilibrium dialysing system with 1.5 ml capacity was used. Samples were diluted (1: 14 volumetric ratio, 0.1 ml of sample + 1.4 ml of double deionized water) and dialysed for 5 hours in 2 L of deionized water, using 500 MWCO membrane. The deionized water for dialysis was changed every hour.

Two GCPQs with different characteristics were fragmented and the reaction was sampled and quenched at the predetermined times. The samples were purified and stored in the freezer for further analysis. Reaction was sampled at different times in order to see the change in the size of fragments with time and to establish the relationship between the fragmentation conditions (fragmentation time, pH, nitrous acid- polymer molar ratio) and the size of fragments. This would allow optimisation of the fragmentation to obtain desired size of fragments (<1000 Da).

Table V*: Characteristics of polymer batches, used for fragmentation*

POLYMER BATCH	Mw (Da)	PDI	%P	%Q
GCPQ B3E	21000	4.9	34.6	14.6
GCPQ Q23	23000	2.3	4.0	3.0

4.3.2.3.1 MALDI TOF

The instrument used for analysis was Applied Biosystems Voyager- DE Pro Biospectrometry Workstation. Samples were prepared with sinapinic acid, used as a matrix, to obtain 10 mg/ml concentration in the mixture of water and acetonitrile, with adition of trifluoroacetic acid (50:50 mixture of water and acetonitrile + 0.1% TFA). 1 µL of sample matrix mix were spotted on a stainless steel plate. After analysis, data was processed with DataExplorer processing software.

The analysis was preformed twice in order to obtain more information about the fragmentation process and the polymer's structure.

5. Results and discussion

5.1 Synthesis and characterization of GCPQ

3 batches of the polymer were synthesized, using the in- house protocol, described previously (*Chapter 4.1.1*). Synthesized polymers were then characterised using Gel permeation chromatography MALLS and ^{1}H-NMR to determine characteristics, showed in the table below.

Table VI*: Characteristics of three different polymer batches synthesized*

BATCH	Mw (Da)	Mn (Da)	PDI	% P	% Q
GCPQ 1	13690	10130	1.352	10	8.09
GCPQ 2	8557	6314	1.355	2.48	7.9
GCPQ 3	24890	20110	1.238	19.88	11.24

The example of ^{1}H-NMR spectrum is showed below, with the peaks assigned. The degree of palmitoylation and quaternization were calculated as mentioned beforehand (*Chapter 4.1.2.2.1*).

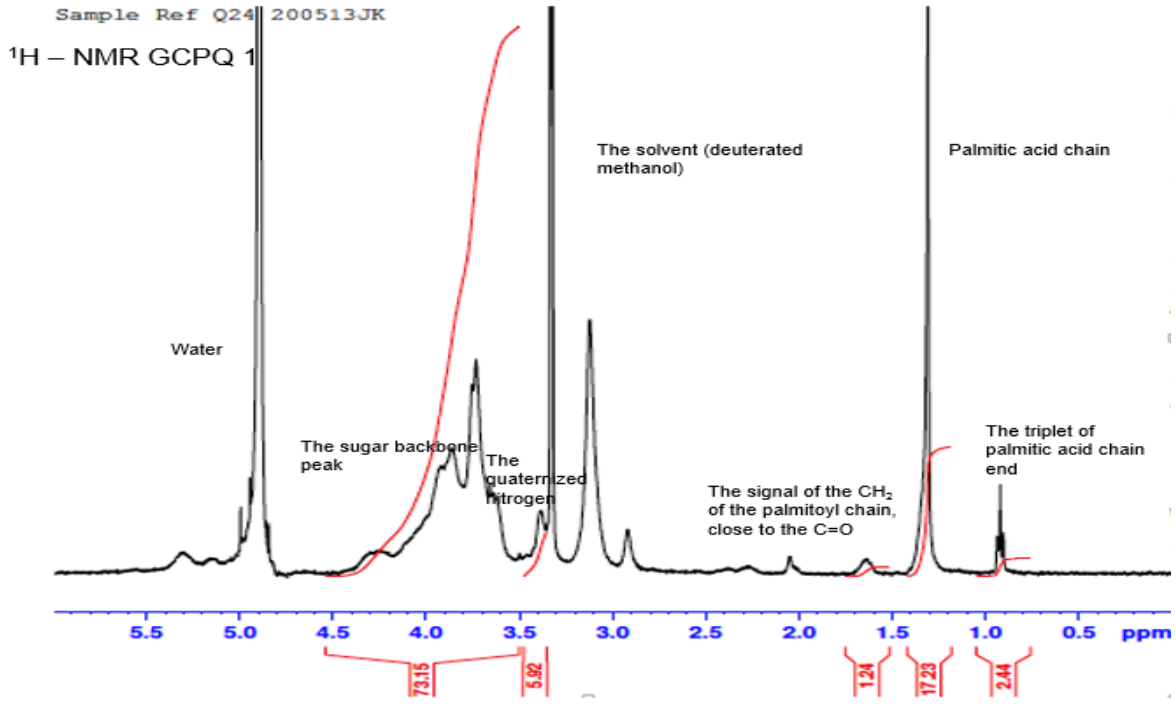

Figure 9*: ^{1}H-NMR spectrum of GCPQ1 with assigned peaks*

The molecular weight and the polydispersity index of polymers were determined using GPC MALLS.

The dn/dc value was determined for each polymer separately and then used for the calculation of the molecular weight (Mw and Mn) and the polydispersity index. All the characteristics of three polymer batches are summarized in the *Table VI*, and the molecular weights of the polymers are slightly different from the expected ones (using the synthesis protocol explained in *Chapter 4.1.1*) probably due to the scale up- the protocol was initially written for 100 mg of GC and each batch of polymer for this project was synthesized using higher amount of the starting material (GC).

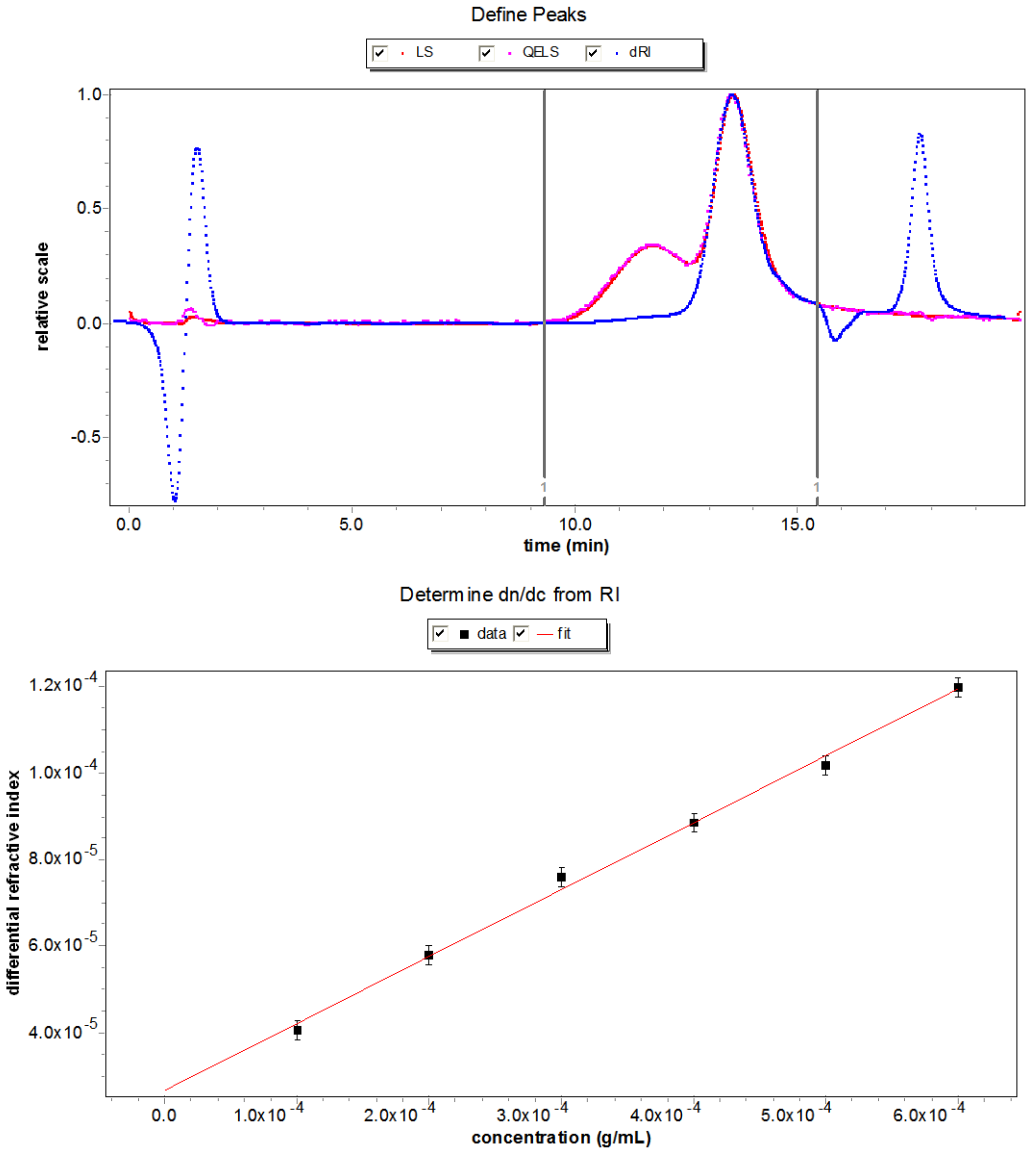

Figure 10, Figure 11*: Example of GPC MALLS and dn/dc result of GCPQ1*

5.2 Formation and characterization of GCPQ nanoparticles

Polymer nanoparticles were prepared in different solvents, using previously described procedure (*Chapter 4.2.1*). 3 batches of the synthesized polymers with different characteristics (molecular weight, degree of palmitoylation and quaternization) were used (characteristics are showed in the *Table VI*).

The average particles size **(Z-average)** of different polymers in different solvents was determined and compared to establish the relationship between polymers' characteristics, solvents' characteristics and the average size of the nanoparticles.

5.2.1 GCPQ 1

This batch of the polymer has the characteristics of intermediate degree of palmitoylation and quaternization, compared to other two batches of the polymer used. The polymer is the second biggest one, with the molecular weight of 13690 Da.

The more detailed look at the *Graph i* reveals that this polymer forms the smallest particles in water, the average particles size is increasing in SGF and it reaches maximum in PB. The degree of palmitoylation of the polymer (10%) is probably not high enough for this polymer to aggregate in water, making Z-average smaller. In SGF, the ionic strength of the solvent is higher due to the addition of sodium chloride and the pH is low, around 1.2. High ionic strength affects zeta potential and causes it to decrease, while low pH causes the increase in zeta potential. In PB, the pH is higher, so the zeta potential is decreasing. When zeta potential becomes higher than around 30mV or lower than around -30mV, the particles are stable. When the value of the zeta potential is in between, repulsion forces between particles become smaller and particles tend to aggregate and flocculate, which causes the increase in particles size (Z-average). It is possible that the particles in SGF and PB are aggregating or flocculating, causing higher Z-average values, while in water the polymer is soluble. The charge density of the polymer also has an important impact on the particles size. [29, 32, 33]

In water, only one analysis was conducted due to the lack of the sample. Two tailed unpaired t-test was conducted using Prism 6.0 statistics software, to compare the Z-average of the particles in SGF and PB. The results showed there is no significant difference in the Z-average of the polymer nanoparticles between SGF and PB ($p=0.2538$).

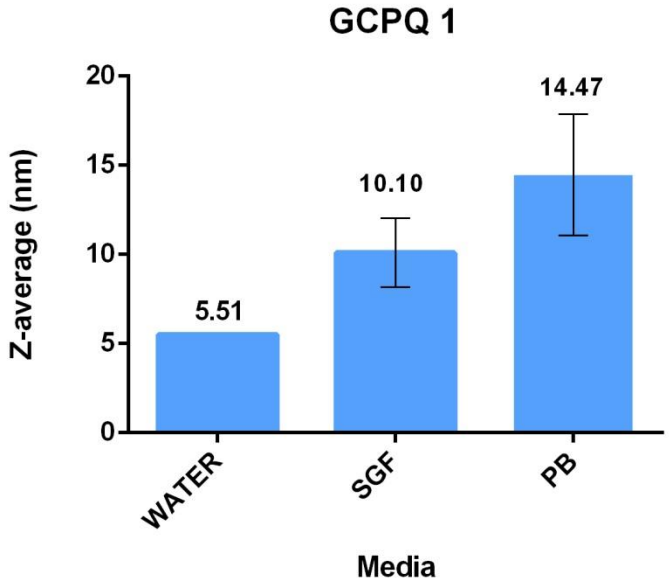

Graph i*: Z-average of GCPQ1 nanoparticles in different solvents with SD error bars and Z-average marked*

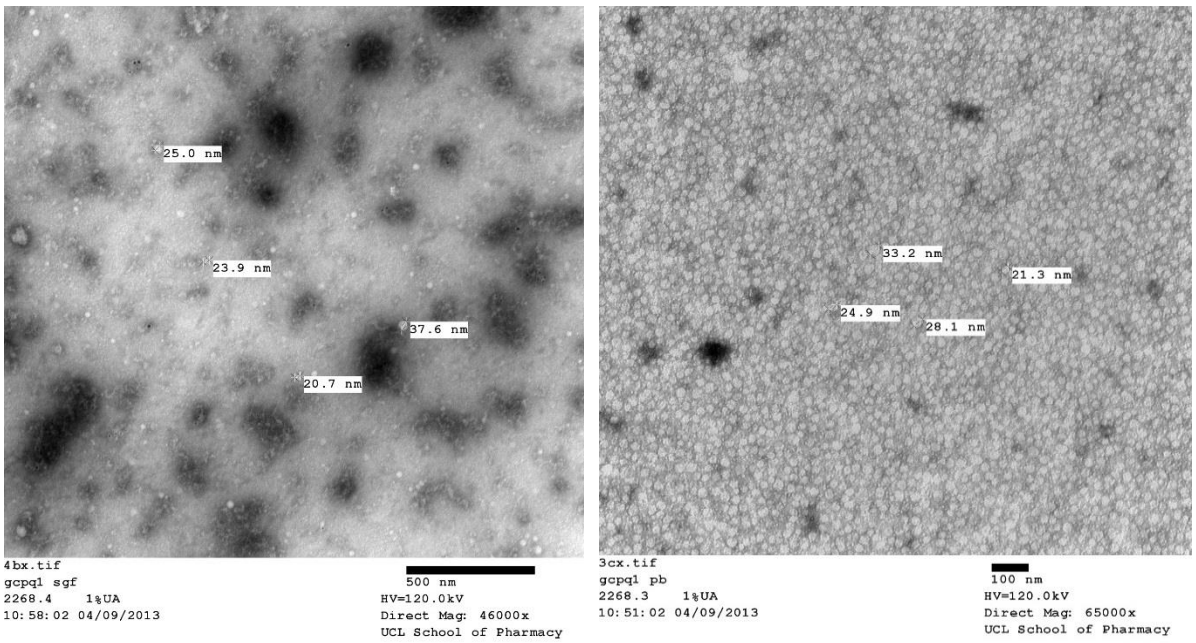

Figure 12, Figure 13*: TEM images of GCPQ1 nanoparticles in SGF (left) and PB (right)*

TEM images of the polymer in both solvents show bigger particles than the DLS results. The size distribution by intensity, obtained with the DLS, showed the presence of 2 populations of particles in each solvent- a population of small particles and the population of big particles, meaning the solutions were polydisperse. The population of the small particles contained

more particles compared to the bigger particles population, in all solvents. DLS result is an average size of the particles, based on both particles populations. A closer look to the TEM images reveals the particles are formed nicely, having a round shape.

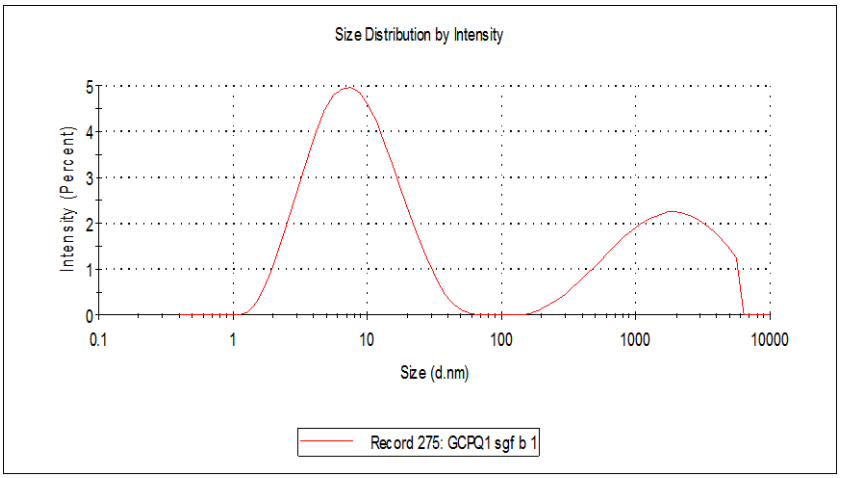

Figure 14*: The size distribution by intensity of GCPQ1 in SGF, showing polydisperse solution*

5.2.2 GCPQ 2

This batch of the polymer is the low molecular weight polymer, with the low degree of palmitoylation (2.48%) and quaternization.

The result of this low palmitoylated GCPQ is very similar to previous one. The particles in water and SGF are of the similar size while particles in PB are bigger (*Graph ii*). This polymer has a really low degree of palmitoylation and it does not form aggregates in water and SGF. In PB, the pH is higher and zeta potential starts decreasing, at some point it reaches the value when particles start aggregating.

One way ANOVA test, used to compare Z-average of the particles in water, SGF and PB showed significant difference ($p<0.05$) in Z-average between all three solvents, except for the particles in water and SGF, which are not significantly different size ($p>0.05$).

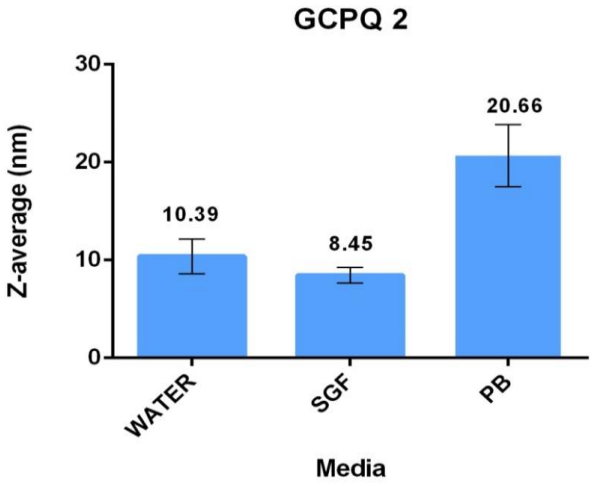

Graph ii*: Z-average of GCPQ2 nanoparticles in different solvents with SD error bars and Z-average marked*

TEM image of polymer in water (*Figure 15*) shows nicely shaped round particles with the size ranging from 16 up to 27 nm, with also smaller and bigger particles seen on the image. Images in SGF and PB are much more chaotic. On both images black dots, smaller than anything else, appear. It is possible that those are copper particles, as the grids used for TEM are made of copper. Image of particles in SGF (*Figure 16*) shows bigger aggregates of particles, while the DLS results measured particles of much smaller size. In PB (*Figure 17*), it seems like there are also some aggregates as well as individual particles present. Probably also salts present in both SGF and PB have an impact on the particles size and organisation. However, the images in PB and SGF are not very reliable as copper ions seem to be present.

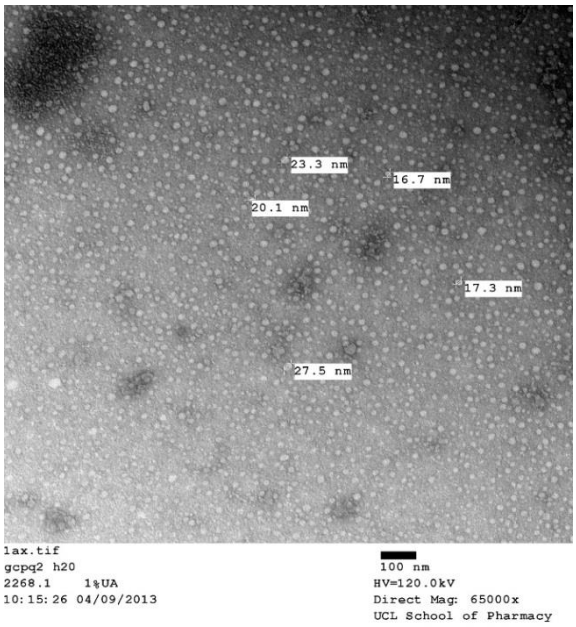

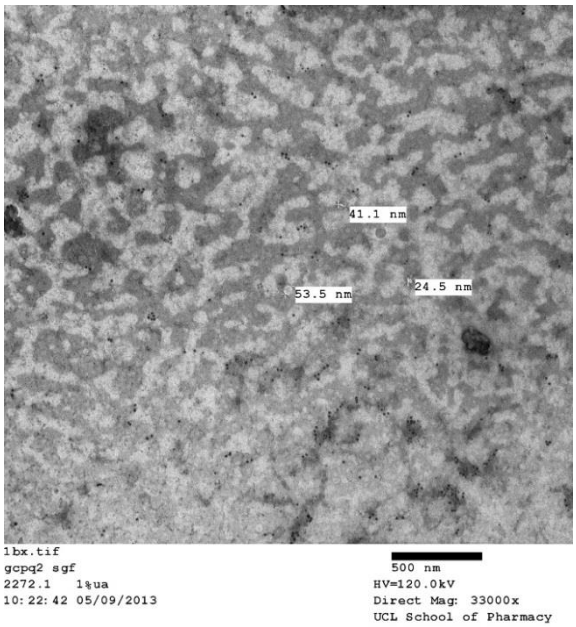

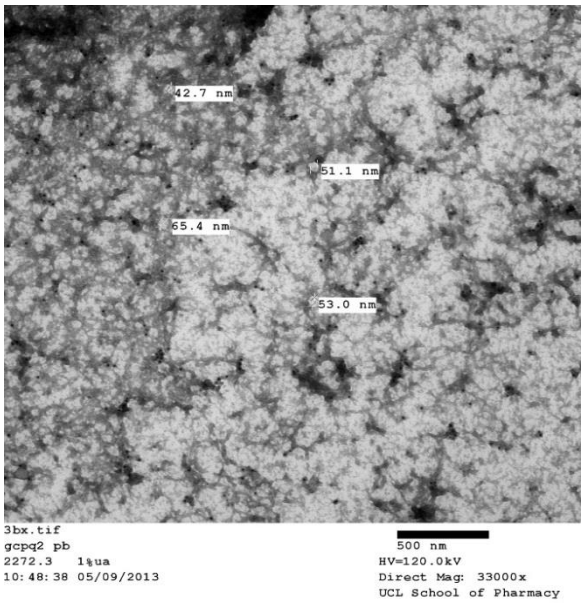

Figure 15, Figure 16, Figure 17*: TEM images of GCPQ2 nanoparticles in water (upper left), SGF (upper right) and PB (lower)*

5.2.3 GCPQ 3

Third batch of the polymer was the high molecular weight polymer with high degree of palmitoylation (19.88%) and quaternization.

High degree of palmitoylation could be the reason for aggregation of polymer particles in water and SGF because of less suitable hydrophilic environment in which hydrophobic palmitic chains cause particle assembling. Also, charge density of the polymer affects the particles size.

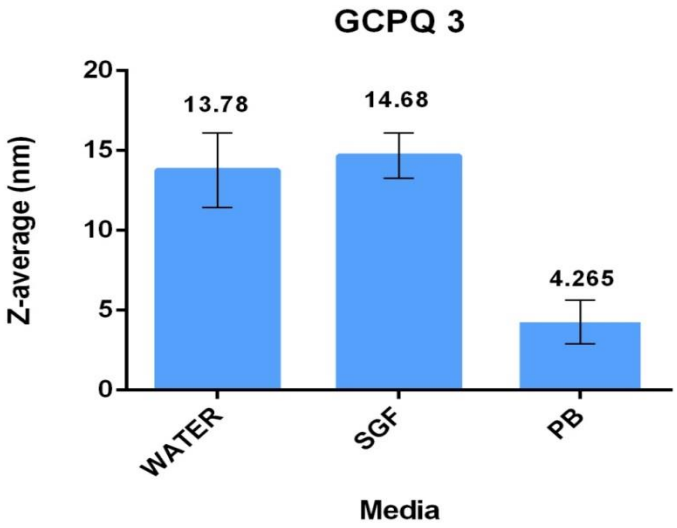

Graph iii*: Z-average of GCPQ3 nanoparticles in different solvents with SD error bars and Z-average marked*

One way ANOVA test, used to compare Z-average of the particles in water, SGF and PB showed there is significant difference ($p<0.05$) in Z-average between all solvents, except of the particles in water and SGF, which are not of significantly different size ($p>0.05$).

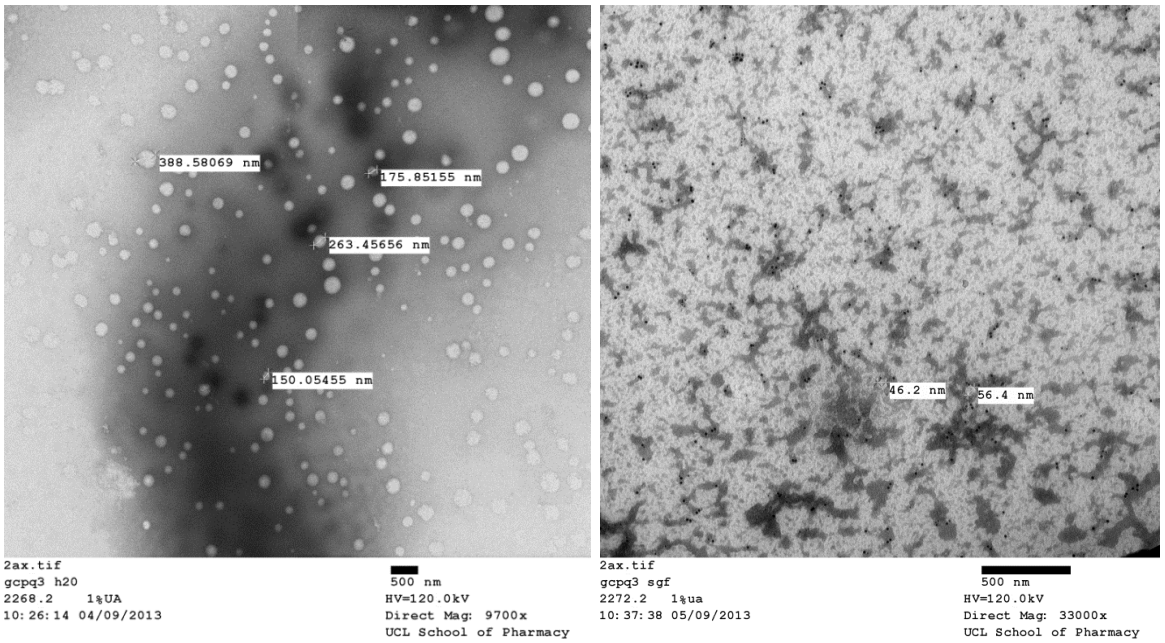

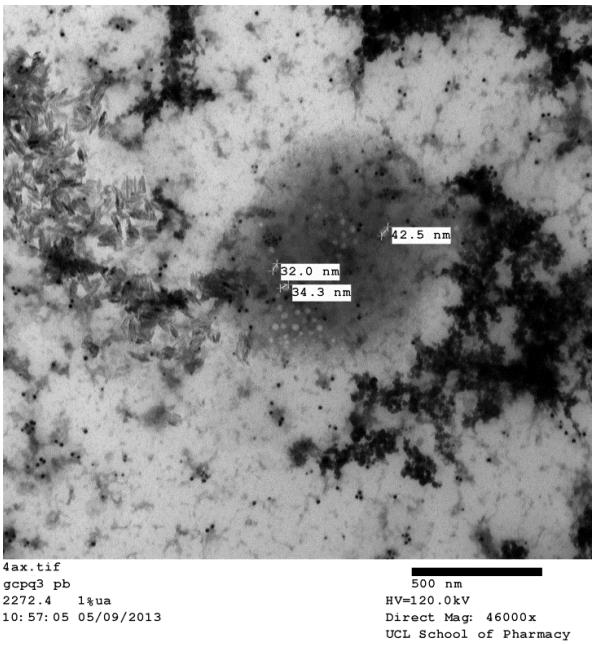

Figure 18, Figure 19, Figure 20*: TEM images of GCPQ3 nanoparticles in water (upper left), SGF (upper right) and PB (lower)*

TEM image of polymer in water (*Figure 18*) shows nicely round shaped particles of the bigger size, up to 390 nm, with also smaller particles seen on the image. Images in SGF and

PB are again much more chaotic. On both images black dots, smaller than anything else, appear. It is possible that those are copper particles, as the grids used for TEM are made of copper. Image of particles in SGF (*Figure 19*) shows bigger aggregates of particles, while the DLS results measured particles of much smaller size. In PB (*Figure 20*), it seems like there are also some aggregates as well as individual particles present. There seem to be also some crystals present in the sample and some other bigger structures, maybe some salts present in both SGF and PB. The TEM images show the biggest particles forming in water, followed by SGF and PB, which is consistent with the DLS results. However, the images in PB and SGF are not very reliable as copper ions seem to be present.

One way ANOVA test with Tukey's multiple comparisons between all three polymers in SGF and PB was conducted. The test showed that there is no significant difference ($p>0.05$) between particles size of GCPQ 1 and GCPQ 2 in both solvents and between GCPQ 1 and GCPQ 3 in both solvents. This was expected, because GCPQ 1 was the polymer with intermediate degree of palmitoylation and quaternization and as such it was close to both of other polymers regarding mentioned characteristics. On the other hand, GCPQ 2 was low palmitoylated and GCPQ 3 was high palmitoylated, making the difference in polymers behaviour bigger.

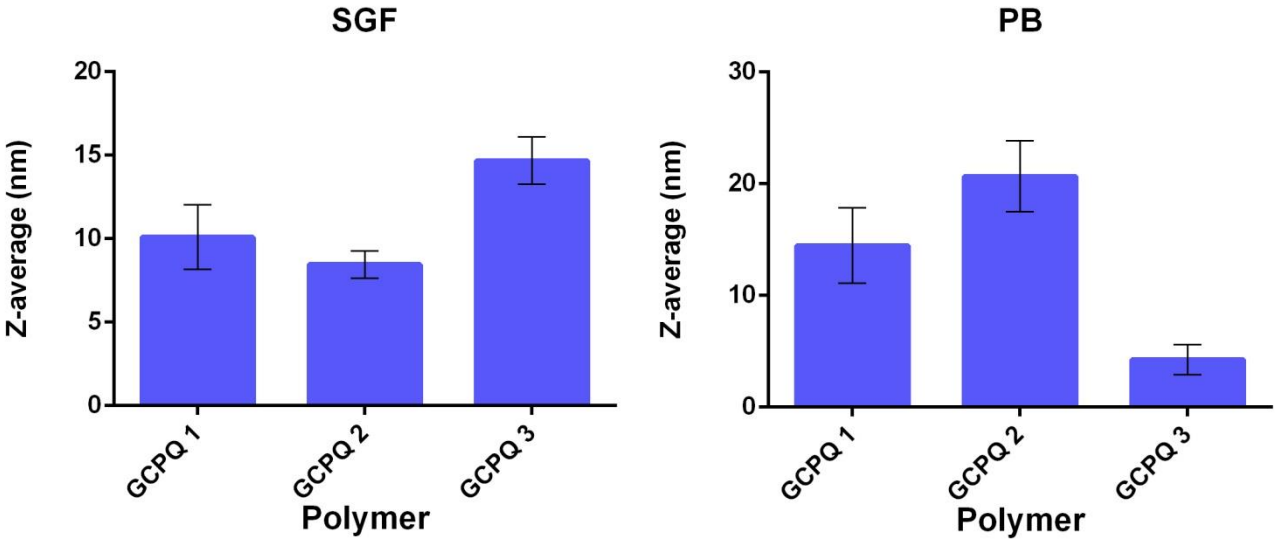

Graph iv, Graph v*: Z-average of polymers nanoparticles in SGF and PB with SD error bars*

In SGF, the particles size is increasing with the degree of palmitoylation, while in PB the average particles size is decreasing with the degree of palmitoylation.

WATER: after %P reaches certain value, particles will start aggregating because of unsuitable environment; before that polymer forms smaller particles.

SGF: The decrease of the pH value increases Z-average values. The presence of acid causes the free amino groups present in the GCPQ molecules to become positively charged. Therefore the amount of acid strongly affects the charge density of GCPQ molecules and thus the chain conformation. Addition of NaCl leads to decrease of zeta potential. The reduction of the repulsive potential, favoured by the interaction of the charged amino groups with the anions Cl^- is possibly the cause for this behaviour. This repulsion reduction results in an increased potential of flocculation or precipitation and increase in particle size. [32, 33]

PB: The increase of pH leads to a decrease of the zeta potential for similar salt and polysaccharide concentrations, possibly resulting from a decrease of the charge density of the polymer provoked by the reduction of the concentration of H^+ ions. [32, 33]

Salting out phenomena: When the salt concentration is increased in polymer aqueous solution, some of water molecules solvate the salt ions. This may decrease the number of water molecules available to interact with the charged part of hydrophilic, water soluble part of the polymers, leading to the polymer-polymer interactions, forming polymer coagulate by forming interactions with each other.

The results suggest that the solvent does have some impact on the polymer's behaviour and the formation of nanoparticles, though no significant difference was observed for a polymer in different solvents. The GCPQ is known to form micelles (10-30 nm) in aqueous media [15], which could also be seen on some TEM images. The low palmitoylated polymer seems to form the smallest particles in SGF and the biggest particles in PB. This suggests that the polymers' characteristics, such as degree of palmitoylation and quaternization also have some impact on the polymers' behaviour in different solvents. The low palmitoylated polymer with similar degree of quaternization has more free amino groups compared to high palmitoylated polymer. In SGF, when the pH is low, those free amino groups will get protonated and the charge density of the low palmitoylated polymer will be higher compared to the high palmitoylated polymer. Therefore, the reduction of the zeta potential and the repulsive forces caused by addition of NaCl in SGF and interactions between Cl^- and charged amino groups, will be lower for low palmitoylated polymer and the rise of the average particles size will therefore be lower, compared to high palmitoylated polymer. In PB, the situation is the

opposite- the pH is higher and the amino groups are getting deprotonated due to reduction of H^+ concentration, causing the charge density of the polymer and the zeta potential to decrease. The reduction is bigger for the low palmitoylated polymer with higher concentration of free amino groups and the flocculation potential is therefore higher. [32, 33]

5.3 Fragmentation of GCPQ

5.3.1 GPC MALLS

The polymer was fragmented with nitrous acid, following previously described protocol (*Chapter 4.3.1*). The reaction was sampled at different time points (1 hour, 2 hours, 6 hours and 8 hours) and the samples were analysed with GPC MALLS to get the insight in the reaction kinetics and to observe the expected change in the molecular weight of the undegraded polymer with time. The undegraded polymer was used as a standard.

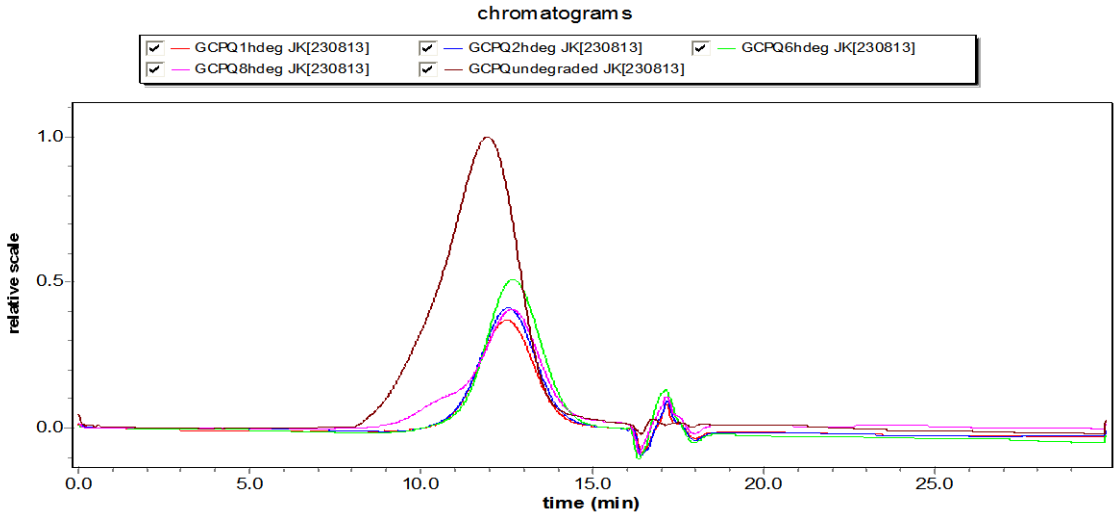

Graph vi*: The retention time of the polymer at the different time points of the fragmentation*

On the graph showing retention time versus fragmentation time it is possible to see how the retention times of different time points are increasing with increasing fragmentation time. This indicates the decrease in the size of polymer, which suggests the fragmentation is happening. It is impossible to determine the molecular weight of polymers, belonging to certain time points, because analysed samples do not consist of pure polymer but are a mixture of polymer fragments and reactants added in the process of fragmentation. Therefore, determining dn/dc value, needed for molecular weight calculation, is not possible. Retention time is increasing with fragmentation time, so the conclusion is that the size decrease is

present and fragmentation is happening, faster at the beginning than later (the curve is steeper at the beginning).

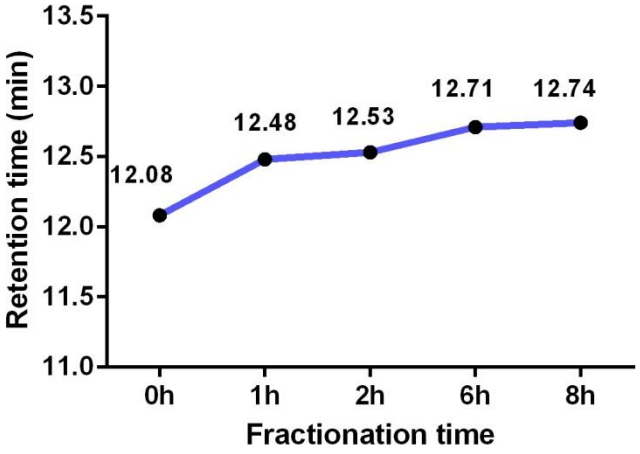

Graph vii*: Retention time versus fractionation time for different time points of the polymer fractionation*

5.3.3 Mass spectroscopy

5.3.3.1 MALDI TOF

Two polymers with similar molecular weight and very different degree of palmitoylation and quaternization were used (*Table III*). Both polymers were fragmented with the same method, using nitrous acid and the reaction was sampled at the same time points.

Total ion scan was conducted to get the first indication of molecular weight of the fragments forming during the fragmentation reaction and how it changes with time. The analysis was carried out twice for the same polymer and time points to get the better insight to the fragmentation reaction. The conditions and the instruments used were described previously (*Chapter 4.3.2.3.1*).

The presumed structures of fragments are given in the tables. The abbreviations are being used: A for acetylated monomer, D for deacetylated monomer, P for palmitoylated monomer, Q for quaternized monomer, M for 2, 5-anhydro-D-mannose. G represents glycol group, present on the monomer and the number (2G or 3G) indicates the number of glycol groups (every monomer can either have or not one glycol group).

5.3.3.1.1 GCPQ B3E

Below the MALDI TOF spectrum of undegraded polymer is showed (*Figure 21*), with the base peak marked.

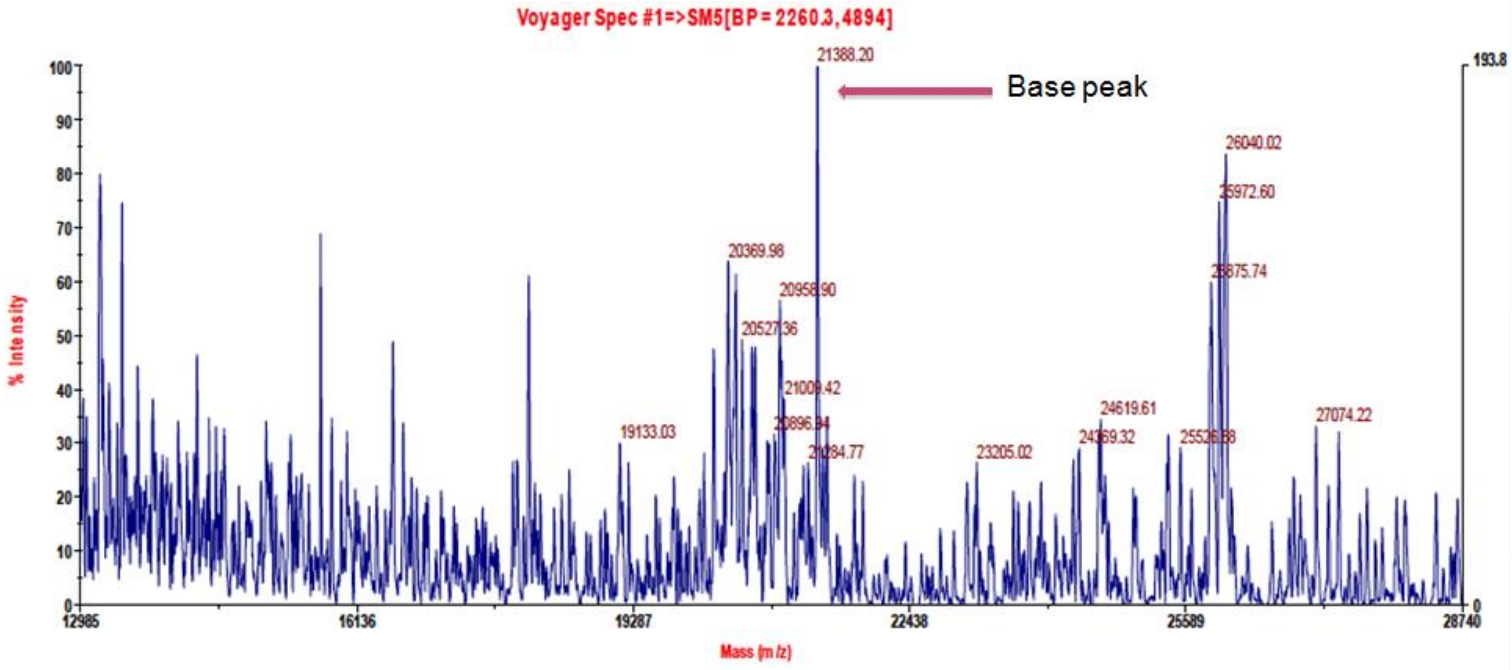

Figure 21*: MALDI TOF spectrum of undegraded GCPQ B3E*

There are many different fragments occurring, but the most abundant fragment (base peak) is at 21388.2 m/z. This polymer had a very high PDI, so it was expected to see many different polymer chains already before the fragmentation. The ion scan is only showing the species between 13000 and 29000 m/z. It is possible that there are also polymers with higher and lower m/z and additional ion scan for broader area should be taken.

After 1 hour of fragmentation , it is possible to see the presence of fragments with smaller m/z. The first spectrum (*Figure 22*) shows peaks between 350 and 2840 m/z. The most abundant peaks are around 450 m/z, which is also the base peak. The structure of the base peak is presumably (A-M-G) K^+, which is adduct of acetylated monomer and the M- end, formed after the cleavage of the glycosidic bond, with potassium. The *Table* VII shows some of the assigned peaks with their presumed structure, centroid mass, charge and relative intensity.

Table VII*: Assigned peaks with presumed fragment structure and relative intensity*

FRAGMENT STRUCTURE	CENTROID MASS	CHARGE	RELATIVE INTENSITY
$(Q\text{-}M\text{-}G)H_2O$	432.353303	+1	64.94
$(A\text{-}M\text{-}G)Na^+$	433.351611	+1	24.68
$(M\text{-}D\text{-}2G)K^+$	452.367965	+1	21.23
$(D\text{-}D\text{-}M)H^+$	488.260879	0	34.04
$(Q\text{-}Q\text{-}M)Cl^- NO_2^-$	656.235622	0	12.53
$(Q\text{-}D\text{-}M\text{-}3G)Cl^-$	698.007411	0	12.51

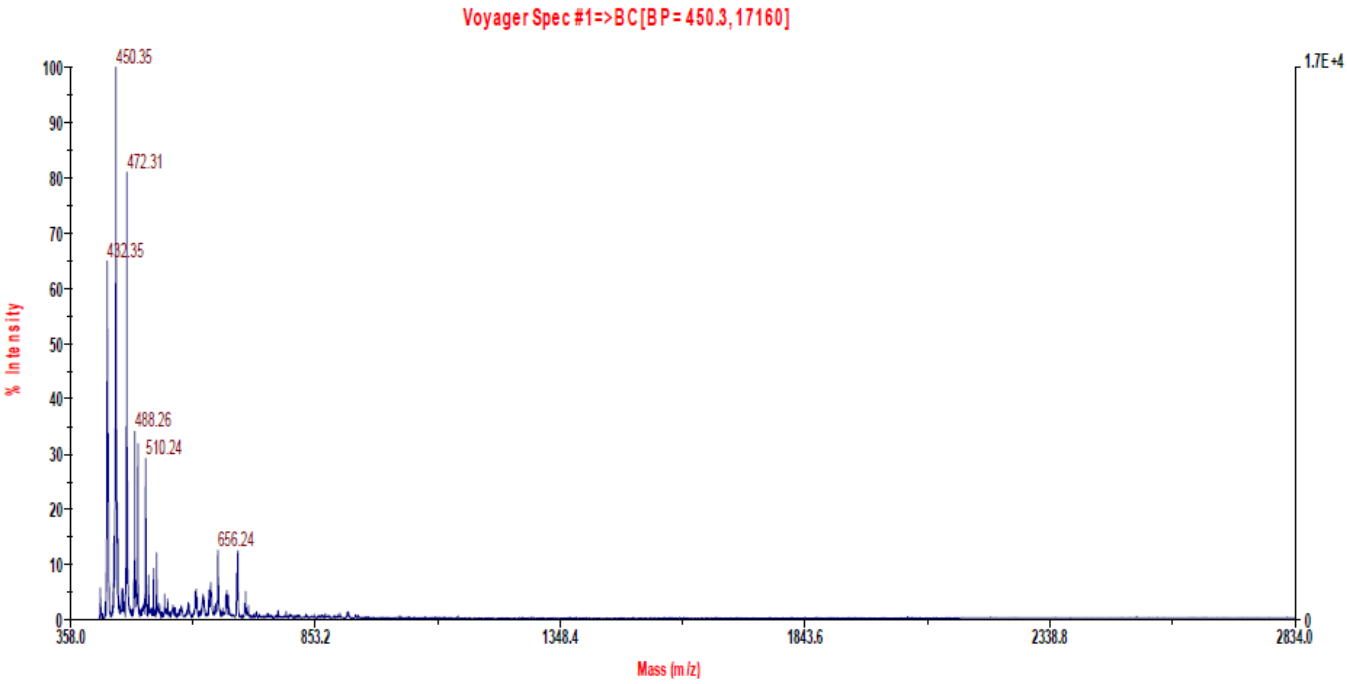

Figure 22*: MALDI TOF spectrum after 1 hour of fragmentation of GCPQ B3E*

The second spectrum of the same polymer and the same time point shows the peaks between 5000 and 30.000 m/z. The most abundant fragments on this spectrum are the ones with lower molecular weight (10.000 m/z and below) - with the rise of the molecular weight the abundance of fragments is falling, which suggests that the polymer chains of high molecular weight are getting fragmented, resulting in the formation of fragments with lower m/z.

From these spectra we can conclude that there is some fragmentation of the polymer happening already during the first hour, but there are still undegraded chains of the polymer present. Abundance of the undegraded polymer is falling with time while abundance of the smaller fragments, forming during the fragmentation, is rising.

After 6 hours of fragmentation, the abundance of fragments with smaller m/z continues to rise. The first spectrum (*Figure 23*) shows the peaks between 370 and 1434 m/z. The most abundant peaks are around 418 m/z, which is also the base peak. The structure of the base peak is presumably P-H^+, adduct of palmitoylated monomer with hydrogen. The *Table* VIII below shows some of the assigned peaks with their presumed structure, centroid mass, charge and relative intensity.

Table VIII: *Assigned peaks with presumed fragment structure and relative intensity*

FRAGMENT STRUCTURE	CENTROID MASS	CHARGE	RELATIVE INTENSITY
$(A\text{-}M)K^+$	406.3311064	+1	13.49
$(Q\text{-}M)NO_2^-$	414.343236	0	15.94
$(A\text{-}M\text{-}G)Na^+$	434.328597	+1	44.31
$(A\text{-}M\text{-}G)K^+$	450.315173	+1	62.05
$(A\text{-}M\text{-}2G)H_2O$	472.329112	0	36.13
$(A\text{-}Q\text{-}M\text{-}G)Cl^-$	695.013934	0	4.59

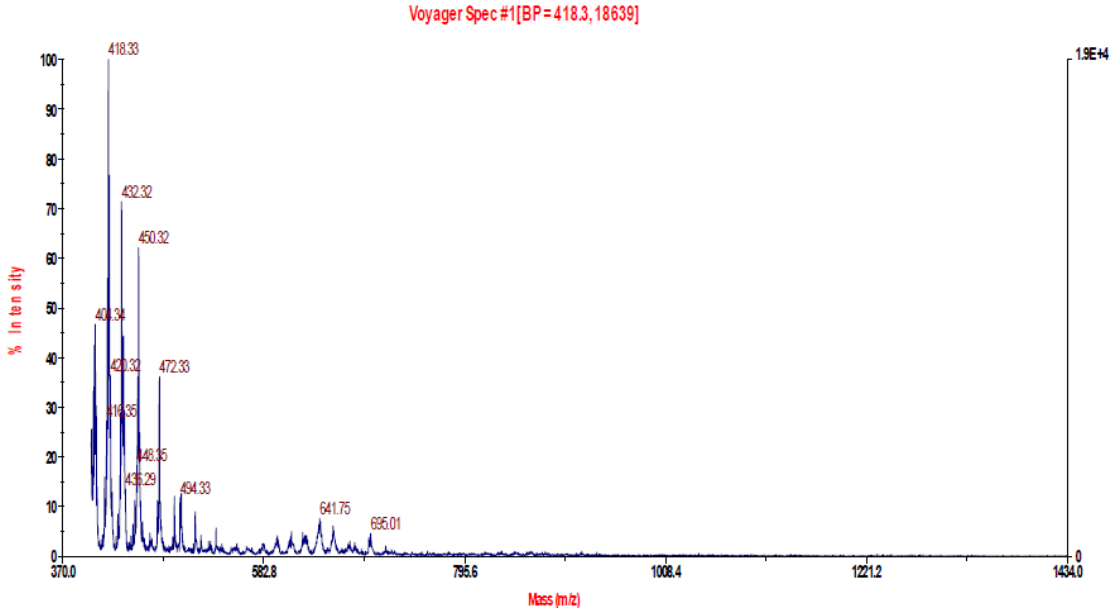

Figure 23*: MALDI TOF spectrum after 6 hours of fragmentation of GCPQ B3E*

The second spectrum (*Figure 24*) shows peaks between 600 and 5500 m/z. The base peak is at 613.69 m/z, with the structure of (A-A-M-G). The *Table IX* below shows some of the assigned peaks with their presumed structure, centroid mass, charge and relative intensity.

Table IX*: Assigned peaks with presumed fragment structure and relative intensity*

FRAGMENT STRUCTURE	CENTROID MASS	CHARGE	RELATIVE INTENSITY
(Q-D-M-G)Cl^-	609.488571	0	22.23
(P-M-G)H_2O	625.670288	0	28.31
(A-Q-M-2G)Cl^-	695.474967	0	34.31
(A-Q-M-3G)Cl^-	739.557622	0	38.63
(P-P-M-G)	1007.188216	0	36.39

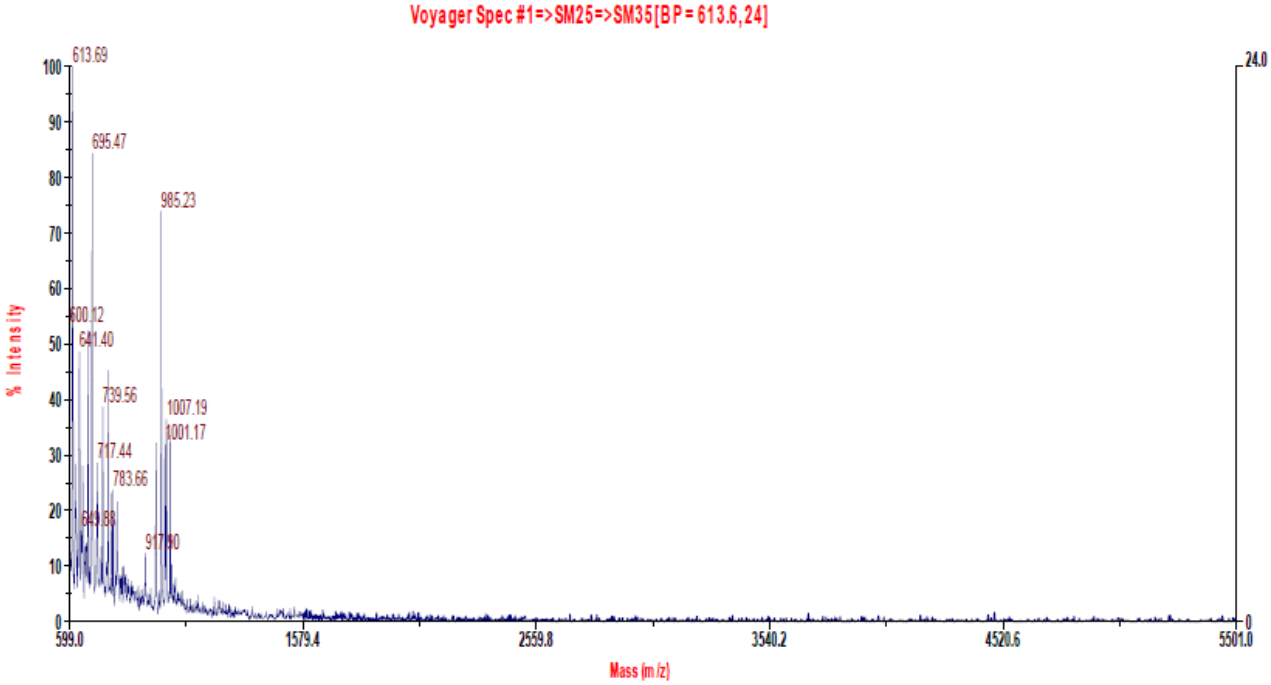

Figure 24*: MALDI TOF spectrum after 6 hours of fragmentation of GCPQ B3E*

The peaks with the greatest abundance belong to the fragments, smaller than 1000 m/z, indicating the fragmentation is taking place. There are no peaks with high abundance present over 1000 m/z, but the total ion scan of the bigger area, up to 23000, should be taken, in order to see if the undegraded polymer is present.

After 24 hours of fragmentation, the undegraded chains of polymer are no longer present as they have fragmented into smaller fragments. The first spectrum (*Figure 25*) shows the peaks between 400 and 811 m/z. The most abundant peaks are around 472 m/z, which is also the base peak. The structure of the base peak could be either (Q-Q)NO_2^- or (P-G)B^+. The *Table X*

below shows some of the assigned peaks with their presumed structure, centroid mass, charge and relative intensity.

Table X*: Assigned peaks with presumed fragment structure and relative intensity*

FRAGMENT STRUCTURE	CENTROID MASS	CHARGE	RELATIVE INTENSITY
$(A\text{-}M)K^+$	406.357781	+1	18.83
$(Q\text{-}M)NO_2^-$	414.368947	0	23.27
$(Q\text{-}M\text{-}G)H_2O$	430.364228	+1	22.01
$(A\text{-}M\text{-}G)Na^+$	434.37671	+1	37.44
$(M\text{-}D\text{-}2G)Na^+$	435.290671	+1	18.83

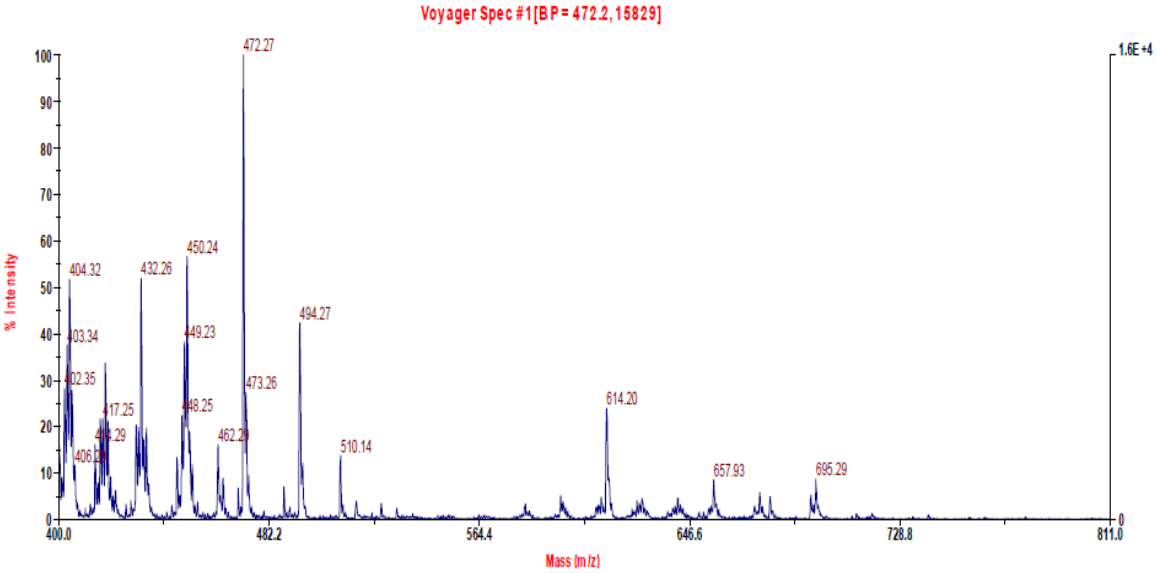

Figure 25*: MALDI TOF spectrum after 24 hours of fragmentation of GCPQ B3E*

The second spectrum shows that there are still polymer fragments present until the 8400 m/z, with higher abundance below 5500. Beyond 8400 m/z and up to 30.000, there is very little polymer fragments present, which indicates that the polymer fragmented successfully and in high extend. Very small amount of undegraded polymer remained and most of it fragmented forming fragments of a few kilo Daltons in size.

These spectra indicate that after 24 hours of fragmentation, there is no undegraded polymer remaining. However, fragments of bigger m/z are still present and the fragmentation is therefore not completed yet.

After 48 hours of fragmentation, the fragmentation reaction seems to be reaching an end. The first spectrum (*Figure 26*) shows the peaks between 380 and 1170 m/z. The most

abundant peaks are around 450 m/z, which is also the base peak. The structure of the base peak is probably (A-M-G) K^+. The *Table XI* below shows some of the assigned peaks with their presumed structure, centroid mass, charge and relative intensity.

Table XI*: Assigned peaks with presumed fragment structure and relative intensity*

FRAGMENT STRUCTURE	CENTROID MASS	CHARGE	RELATIVE INTENSITY
$(A\text{-}M)K^+$	406.357781	+1	18.83
$(Q\text{-}M)NO_2^-$	414.368947	0	23.27
$(Q\text{-}M\text{-}G)H_2O$	430.364228	+1	22.01
$(A\text{-}M\text{-}G)Na^+$	434.37671	+1	37.44
$(M\text{-}D\text{-}2G)Na^+$	435.290671	+1	18.83

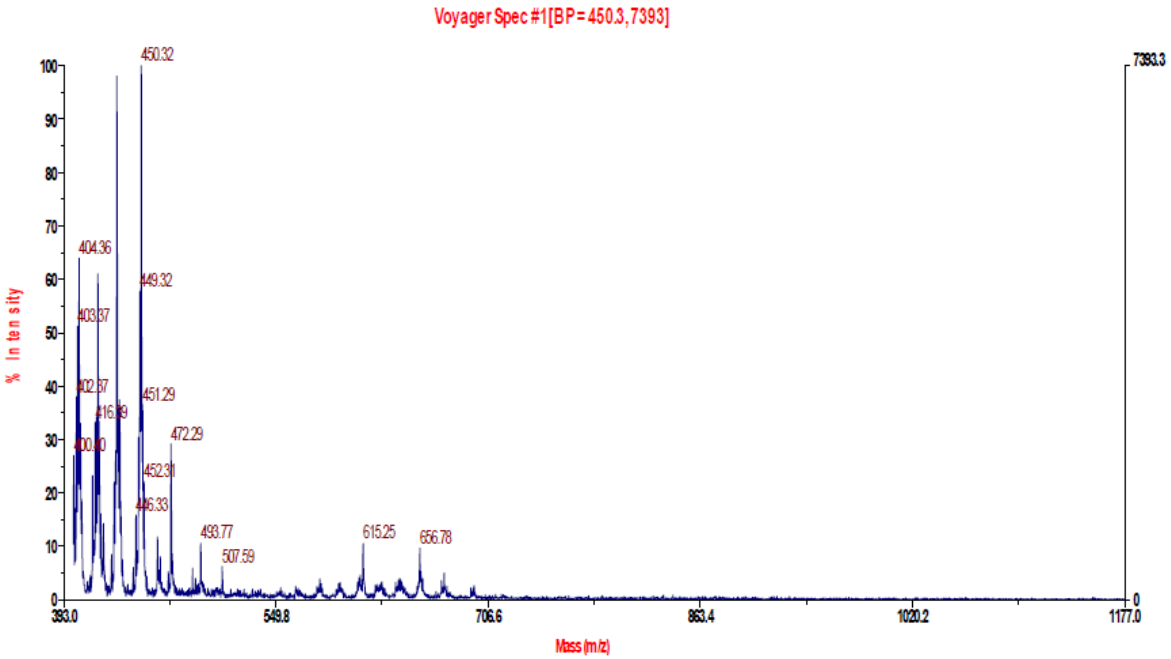

Figure 26*: MALDI TOF spectrum after 48 hours of fragmentation of GCPQ B3E*

The second spectrum (*Figure 27*) shows peaks between 400 and 10000 m/z. The fragments with higher abundance are occuring below 1000 m/z, after that the abundance is falling strongly. There are barely any fragments with the m/z, higher than 2000. This indicates that the polymer got fragmented in great extent, there are no bigger fragments present. Additional scan up to 23000 m/z should be taken to confirm there is no undegraded polymer present, though the second spectrum of 24 hours fragmentation clearly indicates that. The fragmentation of the fragments with m/z 1000 and more could probably be achieved by

prolonging fragmentation time. The *Table XII* below shows some of the assigned peaks with their presumed structure, centroid mass, charge and relative intensity.

Table XII*: Assigned peaks with presumed fragment structure and relative intensity*

FRAGMENT STRUCTURE	CENTROID MASS	CHARGE	RELATIVE INTENSITY
$(Q\text{-}M)Cl^-$	404.900417	0	83.51
(D-M-2G)	413.505803	0	91.23
(A-A-M)	571.668389	0	45.13
M-A-M-2G	600.855516	0	72.81
(A-D-M-2G)	616.200426	0	89.31
(P-M-2G)	649.10827	0	90.21
$(A\text{-}Q\text{-}M\text{-}G)NO_2^-$	660.79193	0	97.84
$(A\text{-}A\text{-}M\text{-}2G)H_2O$	677.865733	0	94.09
$(D\text{-}P\text{-}M\text{-}2G)H_2O$	830.076416	0	48.8
$(P\text{-}Q\text{-}M\text{-}G)Cl^-$	846.180298	0	59.71
$(P\text{-}Q\text{-}M\text{-}2G)NO_2^-$	901.815327	0	57.33
$(A\text{-}P\text{-}M\text{-}3G)H_2O$	918.094666	0	38.35

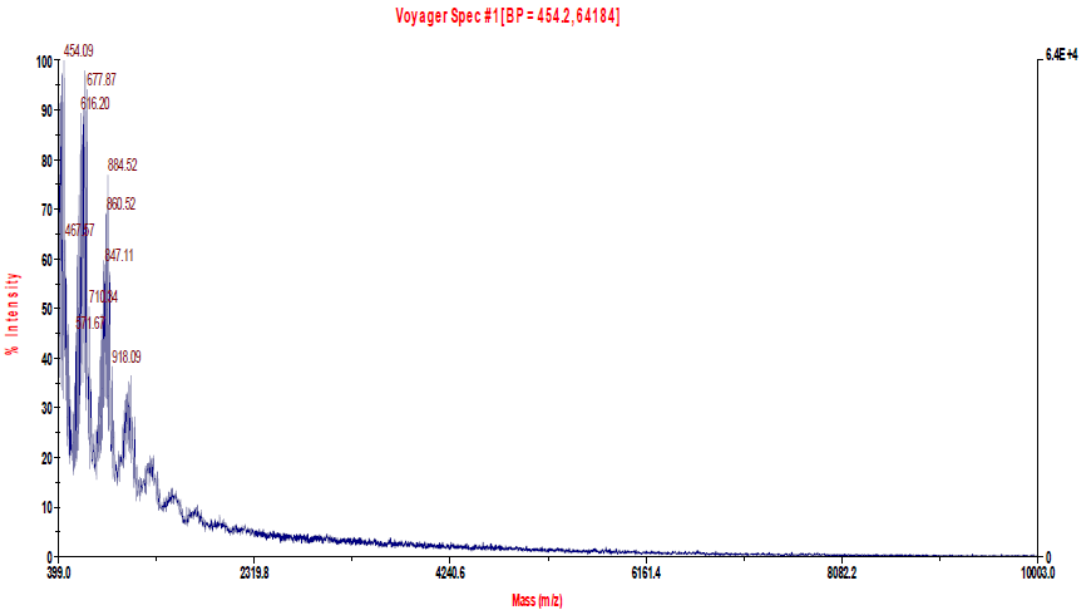

Figure 27*: MALDI TOF spectrum after 48 hours of fragmentation of GCPQ B3E*

5.3.3.1.2 GCPQ Q23

Below the MALDI TOF spectrum of undegraded polymer is showed (*Figure 28*). The molecular weight of this polymer was supposed to be 23000 Da, but the spectrum shows that there are barely any polymer chains, bigger than 12000 m/z. The most abundant chains are with m/z, smaller than 1000. Since the polymer used was not synthesized directly and was stored in the laboratory for few years, it is possible that the storage conditions were not suitable and the depolymerization started, resulting in lower molecular weight. The GPC MALLS of this polymer should be repeated in order to confirm the molecular weight, shown by MALDI TOF. Additionally, the MALDI TOF experiment should be repeated in order to eliminate the option of experimental error. This spectrum is therefore unreliable and cannot be used as a starting point.

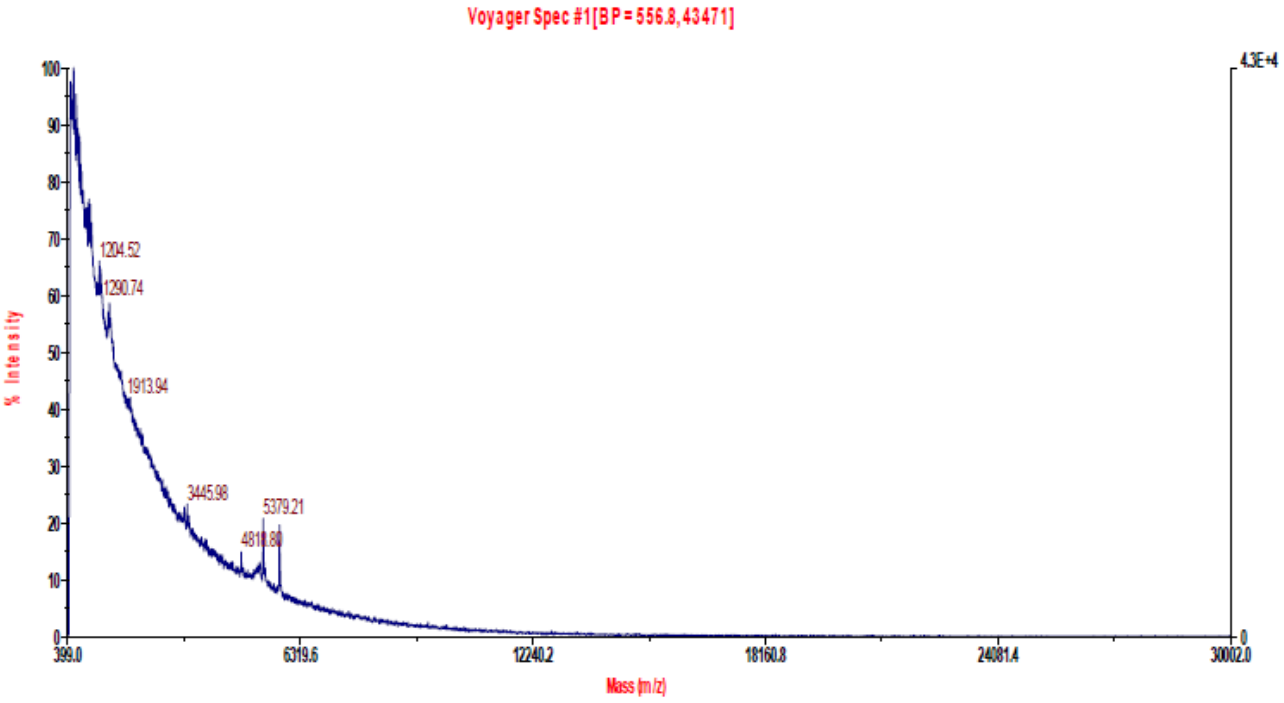

Figure 28*: MALDI TOF spectrum of undegraded GCPQ Q23*

After 1 hour of fragmentation. The first spectrum (*Figure 29*) shows the peaks between 380 and 1600 m/z. The most abundant peaks are around 472 m/z, which is also the base peak. The structure of the base peak is probably (Q-Q)NO_2^- or (P-G)B^+. The *Table XIII* below shows some of the assigned peaks with their presumed structure, centroid mass, charge and relative intensity.

Table XIII*: Assigned peaks with presumed fragment structure and relative intensity*

FRAGMENT STRUCTURE	CENTROID MASS	CHARGE	RELATIVE INTENSITY
$(M\text{-}D\text{-}2G)H_2O$	432.143896	0	28.93
$(A\text{-}M\text{-}G)K^+$	450.099864	+1	67.08
$(A\text{-}A\text{-}M\text{-}G)H^+$	614.962057	+1	14.28
$(Q\text{-}Q\text{-}M)Cl^- NO_2^-$	657.450811	0	6.34
$(Q\text{-}Q\text{-}M\text{-}G)Cl_2$	687.528011	0	8.53

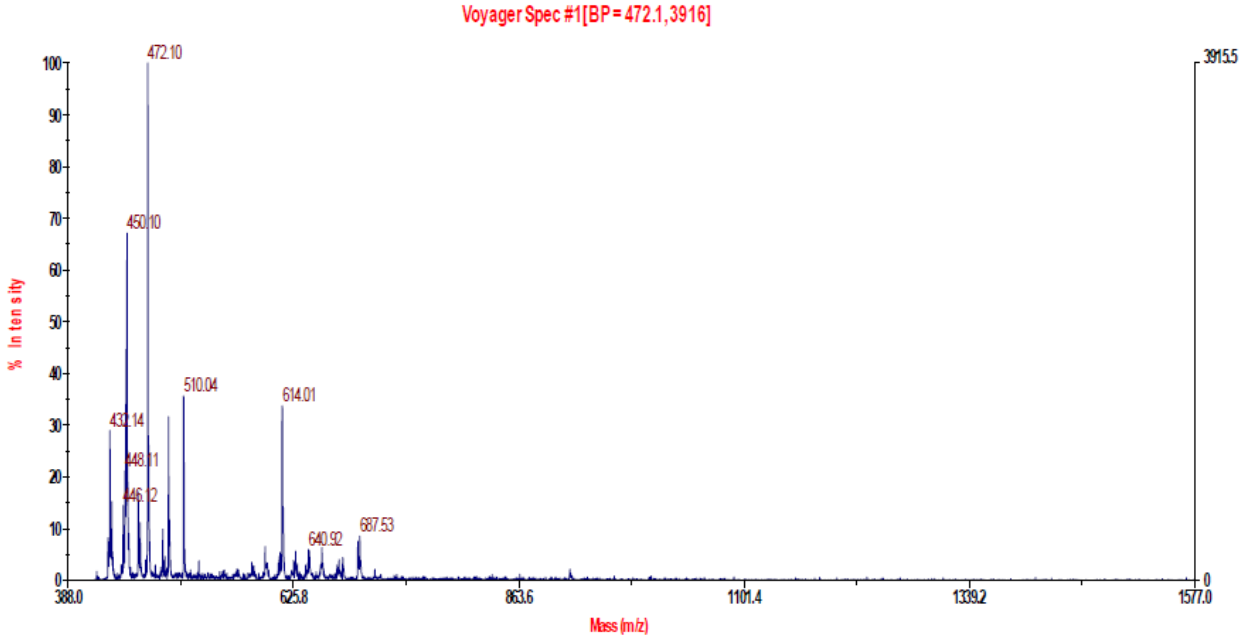

Figure 29*: MALDI TOF spectrum after 1 hour of fragmentation of GCPQ Q23*

The second spectrum (*Figure 30*) shows the fragments with m/z between 5000 and 30000. It is possible to see that there are also polymer chains with m/z 20000 and more present, which indicates that an error occurred during taking the spectrum of undegraded polymer. The abundance of the polymer chains is rising with the fall in m/z ratio, which indicates that there is some fragmentation happening.

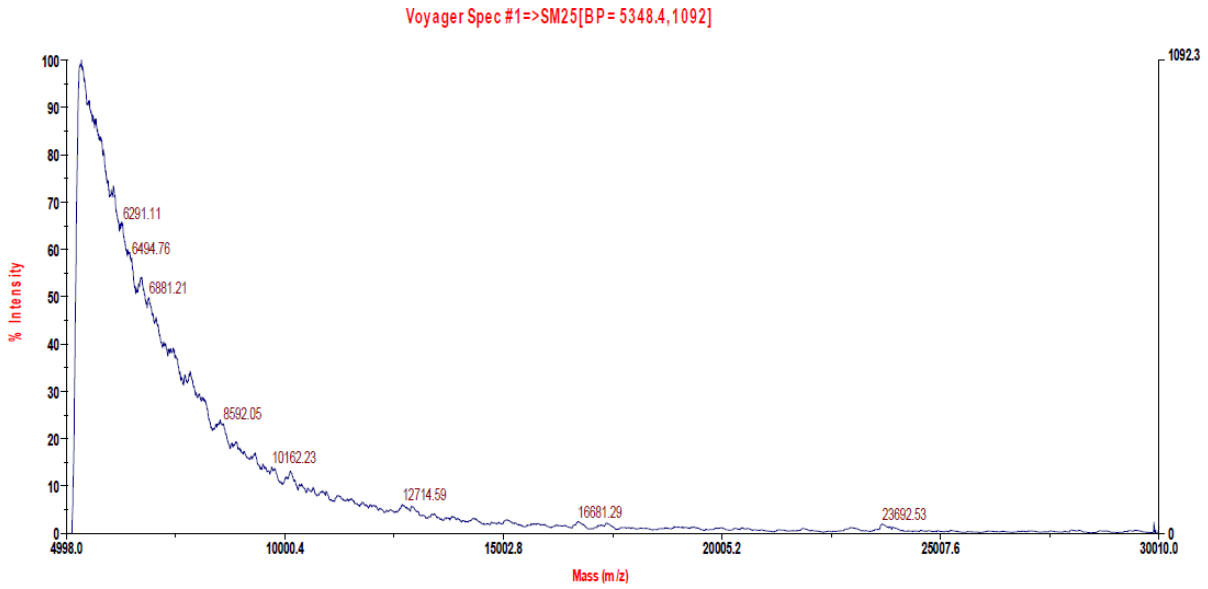

Figure 30*: MALDI TOF spectrum after 1 hour of fragmentation of GCPQ Q23*

From these spectra we can conclude that the fragmentation of the polymer is happening already during the first hour, as the abundance of fragments with high m/z is falling and there are fragments with low m/z forming. There are still chains of undegraded polymer present and the fragmentation time, needed for complete fragmentation of the polymer, is longer.

After six hours of fragmentation. Below, MALDI TOF spectra of the polymer after 6 hours of fragmentation are showed. The first spectrum (*Figure 31*) shows the peaks between 400 and 1100 m/z. The most abundant peaks are around 472 m/z, which is also the base peak. The structure of the base peak is probably $(Q\text{-}Q)NO_2^-$ or $(P\text{-}G)B^+$. The *Table XIV* below shows some of the assigned peaks with their presumed structure, centroid mass, charge and relative intensity.

Table XIV*: Assigned peaks with presumed fragment structure and relative intensity*

FRAGMENT STRUCTURE	CENTROID MASS	CHARGE	RELATIVE INTENSITY
$(M\text{-}D\text{-}2G)H_2O$	432.619466	0	5.86
$(A\text{-}M\text{-}G)K^+$	450.579771	+1	13.53
$(D\text{-}D\text{-}M\text{-}G)H_2O$	548.610309	0	7.16

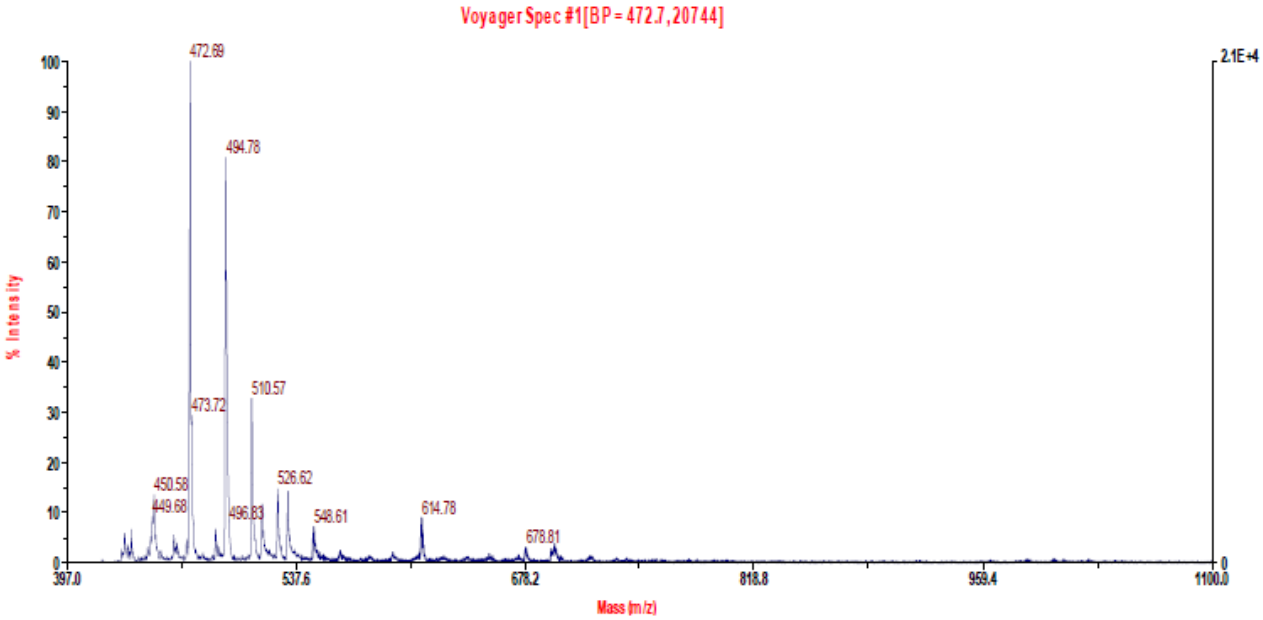

Figure 31*: MALDI TOF spectrum after 6 hours of fragmentation of GCPQ Q23*

The second spectrum (*Figure 32*) shows fragments between 400 and 30000 m/z. The fragments with high abundance are smaller than 1000 m/z, while after 6000 m/z there are barely any fragments, which indicates the successful fragmentation of the polymer. The base peak is (A-A-M-2G), with m/z 658.86. The *Table XV* below shows some of the assigned peaks with their presumed structure, centroid mass, charge and relative intensity.

Table XV*: Assigned peaks with presumed fragment structure and relative intensity*

FRAGMENT STRUCTURE	CENTROID MASS	CHARGE	RELATIVE INTENSITY
(A-M-2G)H_2O	474.459095	0	43.42
(A-A-M)	571.425538	0	42.31
(A-A-M-G)	613.819031	0	74.58
(M-A-M-3G)	643.777905	0	98.45
(A-A-M-2G)H_2O	676.665087	0	76
(D-Q-M-3G)Cl^-	697.734669	0	45.55

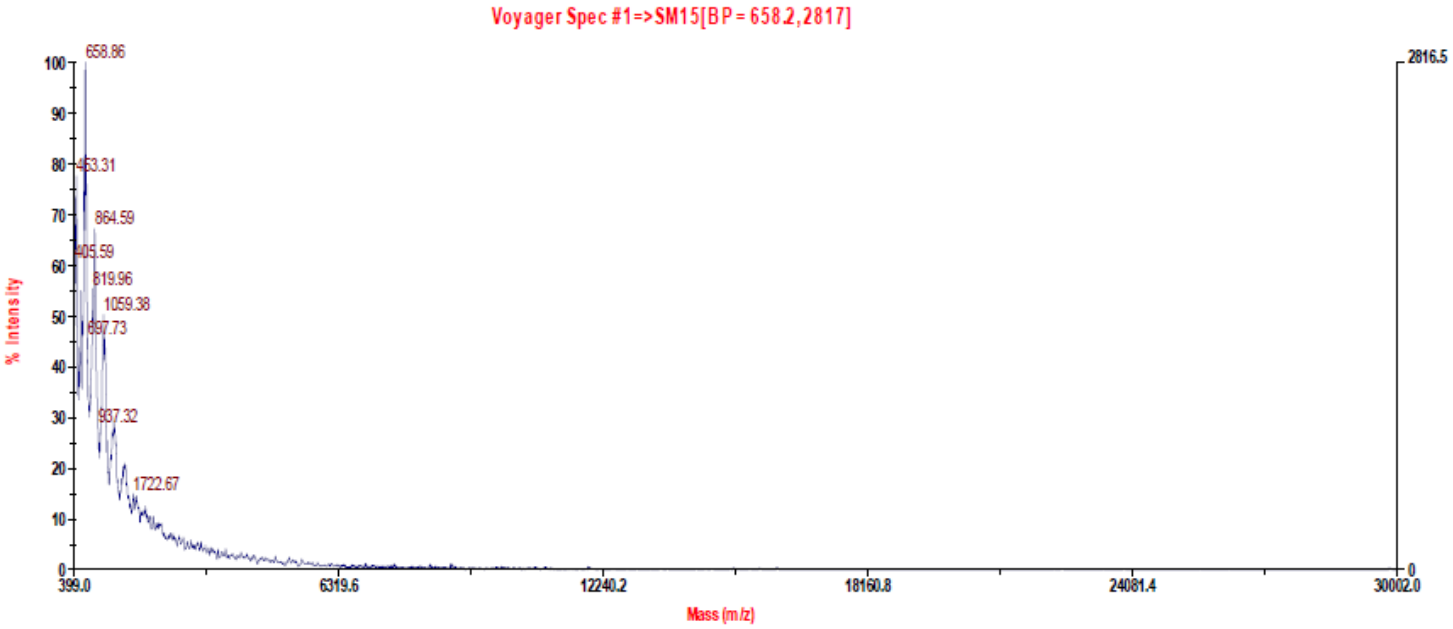

Figure 32*: MALDI TOF spectrum after 6 hours of fragmentation of GCPQ Q23*

After 24 hours of fragmentation. Below, MALDI TOF spectra of the polymer after 24 hours of fragmentation are showed. The first spectrum (*Figure 33*) shows the peaks between 400 and 2000 m/z. The most abundant peaks are around 472 m/z, which is also the base peak. The structure of the base peak is probably (Q-Q)NO_2^- or (P-G)B^+. The *Table XVI* below shows some of the assigned peaks with their presumed structure, centroid mass, charge and relative intensity.

Table XVI*: Assigned peaks with presumed fragment structure and relative intensity*

FRAGMENT STRUCTURE	CENTROID MASS	CHARGE	RELATIVE INTENSITY
(M-D-2G)H_2O	432.560511	0	16.5
(A-M-G)K^+	450.506712	+1	32.05
(A-M-2G)K^+	494.488056	+1	63.64
(A-A-M-G)	614.527605	0	8.5
(A-Q-M-G)Cl^-	696.045281	0	5.41

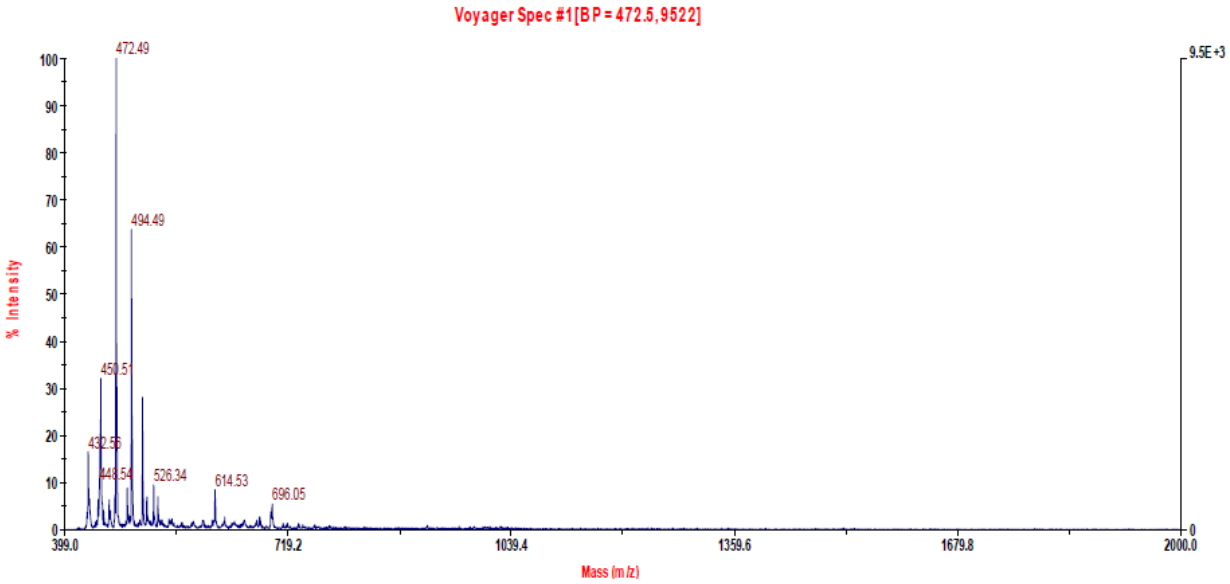

Figure 33*: MALDI TOF spectrum after 24 hours of fragmentation of GCPQ Q23*

The second spectrum shows fragments between 400 and 30000 m/z. The fragments are occurring until the m/z around 6000, after that there are no fragments left, indicating there is no undegraded polymer left. The fragments with the biggest abundance are below 1000 m/z, with the base peak of 653 m/z and the structure (Q-D-M-2G)Cl^-. The *Table XVII* below shows some of the assigned peaks with their presumed structure, centroid mass, charge and relative intensity.

Table XVII*: Assigned peaks with presumed fragment structure and relative intensity*

FRAGMENT STRUCTURE	CENTROID MASS	CHARGE	RELATIVE INTENSITY
(A-A-M)	570.84219	0	68.53
(A-A-M-G)	615.775476	0	96.9
(D-D-M-3G)H_2O	637.376244	0	91.71
(Q-D-M-2G)Cl^-	653.152216	0	98.3
(A-D-M-3G)H_2O	677.307449	0	93.3
(A-Q-M-2G)Cl^-	695.597659	0	51.08
(P-D-M)H_2O	742.061038	0	26.75
(P-D-M-G)H_2O	786.364808	0	34.24
(P-Q-M-2G)NO_2^-	901.245073	0	53.59

After 48 hours of fragmentation. Below, MALDI TOF spectra of the polymer after 48 hours of fragmentation are showed. The first spectrum (*Figure 34*) shows the peaks between 400 and 2000 m/z. The most abundant peaks are around 472 m/z, which is also the base peak. The structure of the base peak is probably $(Q\text{-}Q)NO_2^-$ or $(P\text{-}G)B^+$. The *Table XVIII* below shows some of the assigned peaks with their presumed structure, centroid mass, charge and relative intensity.

Table XVIII*: Assigned peaks with presumed fragment structure and relative intensity*

FRAGMENT STRUCTURE	CENTROID MASS	CHARGE	RELATIVE INTENSITY
$(M\text{-}D\text{-}2G)H_2O$	432.713012	0	16.16
$(A\text{-}M\text{-}G)K^+$	450.131179	+1	33.55
(A-A-M-G)	614.03718	0	12.67

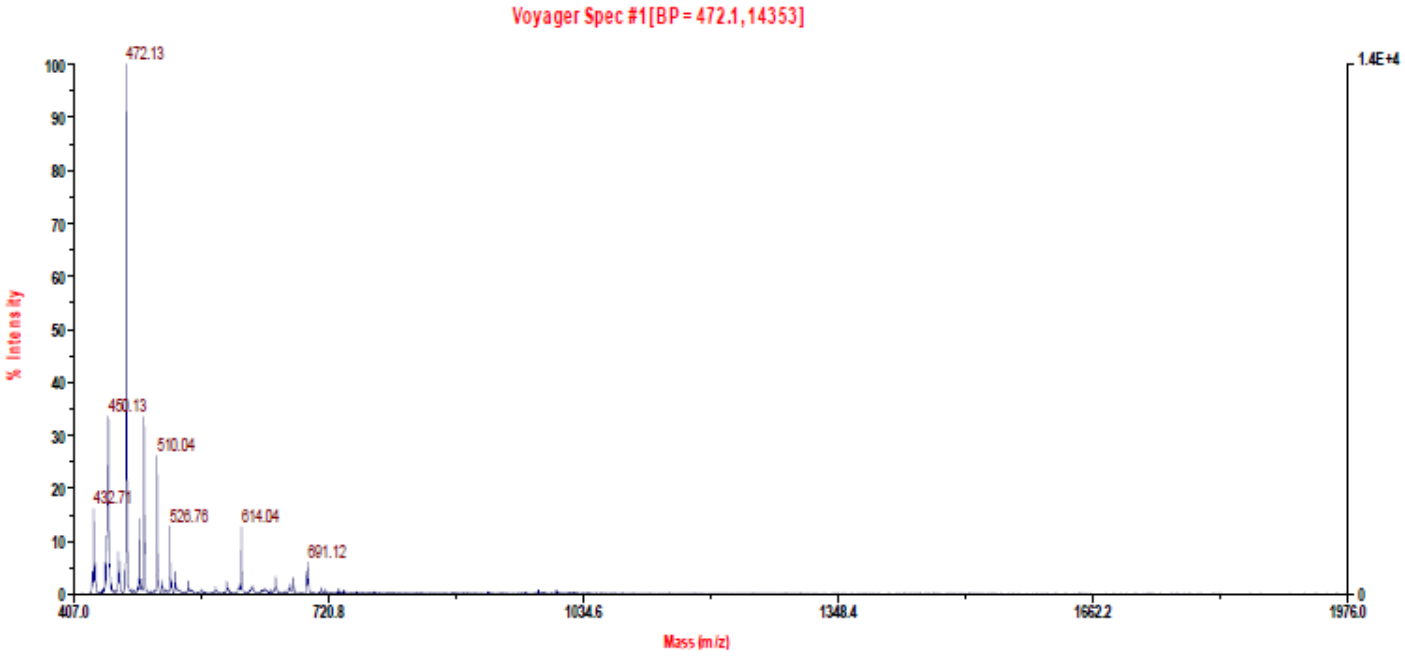

Figure 34*: MALDI TOF spectrum after 48 hours of fragmentation of GCPQ Q23*

The second spectrum shows peaks between 410 and 900 m/z. The most abundant peaks are occurring between 400 and 500 m/z, with the base peak of 432.23 m/z and the structure of $(Q\text{-}M\text{-}G)H_2O$. The *Table XIX* below shows some of the assigned peaks with their presumed structure, centroid mass, charge and relative intensity.

Table XIX*: Assigned peaks with presumed fragment structure and relative intensity*

FRAGMENT STRUCTURE	CENTROID MASS	CHARGE	RELATIVE INTENSITY
$(A\text{-}M)K^+$	406.181602	+1	14.2
$(Q\text{-}M)NO_2^-$	414.330666	0	18.45
$(Q\text{-}M\text{-}G)H_20$	430.330447	+1	17.43
$(A\text{-}M\text{-}G)Na^+$	434.290702	+1	50.46
$(M\text{-}D\text{-}2G)Na^+$	435.167029	+1	28.55
$(A\text{-}M\text{-}G)K^+$	450.311705	+1	91.8
$(M\text{-}D\text{-}2G)K^+$	452.220512	+1	19.64
$(A\text{-}M\text{-}2G)H_2O$	472.267632	0	56.04
$(A\text{-}Q\text{-}M\text{-}2G)Cl^-$	696.101933	0	7.47

The fragments, occurring during the reaction of fragmentation, are mostly dimers, trimers and quatromers, there are also some of the monomers occurring. Most of the fragments are adducts with impurities, present in the sample and originating from the fragmentation reaction, such as K^+, Na^+, NO_2^- and Cl^-. There are also adducts with water and H^+ occurring, which are all very typical for MALDI TOF. The samples were purified, but there are clearly still impurities present. The extent of the dialysis time would be a solution to remove impurities in larger degree, but it would be impossible to completely remove them.

There was a belief based on the literature [11] that in the fragmentation reaction with nitrous acid, glycol group of the polymer remains intact. The results suggest that this is not the case, as in most of the fragments at least one of the glycol groups gets cleaved, forming hydroxyl group on the fragment. The more detailed investigation should be made to confirm this result and the possible solutions to prevent cleavage of the glycol group should be found.

Results suggest there are also some fragments, bearing free amino group (D), where the cleavage of glycosidic bond did not occur. Also, the polymer did not get fragmented to the point where the size of all the fragments would be lesser than 1000 m/z. The solution could be optimization of certain reaction conditions- with extent of the fragmentation time, the increase of the molar ratio between nitrous acid and the polymer in favour of the nitrous acid and with adjusting the pH to 2.9, the size of the fragments should decrease and all the glycosidic bonds should break. However, the reaction should be optimized carefully and wisely.

The most abundant monomer, occurring in the structure of fragments, seems to be the acetylated monomer (A). The palmitoylated monomer (P) does not occur as frequently, as the molecular weight of itself is quite high already. Apart, the size of the palmitoylated group is quite big and the sterical hindrance could prevent attachment of palmitoyl groups to the polymer carbohydrate backbone one next to another. Also, the occurrence of the palmitoylated monomer depends on the degree of the palmitoylation of the polymer- the polymer with high degree of palmitoylation will have higher abundance of palmitoylated monomers in its fragments.

The closer look to the time course of the fragmentation process reveals that there are similar fragments occurring during the whole time of the fragmentation, while their abundance is changing. Also, the results are suggesting that the polymer gets efficiently fragmented with time, causing the abundance of smaller fragments to rise while the abundance of bigger chains is falling. The more detailed scan for the whole range from 500 m/z, which is usually the lowest ratio to scan for in MALDI TOF and up to 21000, which is the molecular weight of the polymer, should be taken, to see if undegraded polymer disappears completely with time.

6. Conclusion

In this master thesis, we were trying to synthesize derivatives of GCPQ with different characteristics and establish the method of fragmentation, suitable for this polymer, which would allow us to obtain fragments of smaller molecular weight. Regarding our aims and objectives, we have:

- Successfully synthesized 3 polymer batches with desired characteristics and determined their characteristics, using ^{1}H-NMR and GPC MALLS
- Successfully formed particles of nano size, using synthesized polymers in different solvents and characterised them using TEM and DLS
- Successfully applied the fragmentation method for GCPQ
- Obtained the first indication of the fragmentation process and the insight into the polymer structure, using established method

Based on our results, we can conclude that following the guidelines for the degradation of glycol chitosan, it is possible to synthesize the polymer of desired molecular weight. The polymer can form particles of nano size in water, SGF and PB and the solvents' and also polymers' characteristics have an impact on the nanopartices formation- especially the degree of palmitoylation and quaternization of the polymer and the ionic strength and the pH of the solvent. The method of fragmentation using nitrous acid does cause the polymer to fragment forming smaller fragments, however further optimisation of the fragmentation method is needed. The GPC MALLS and MALDI TOF results suggest that the fragmentation method is happening faster at the beginning than later (in accordance with Arrhenius equation) and that 48 hours is not enough to completely fragment the polymer to species, smaller than 1000 Da. The change in molar ratio of nitrous acid and polymer, the change of pH or the elevation of the reaction temperature could have an effect on reaction kinetics and size of the fragments.

7. Literature

1. Ijeoma F Uchegbu and Andreas G Schatzlein: Polymers in drug delivery. CRC Taylor and Francis group 2006, United States of America

2. Ijeoma F Uchegbu: Pharmaceutical nanotechnology: Polymeric vesicles for drug and gene delivery. Expert Opinion on Drug Delivery 2006; 3: 629- 640

3. Lalatsa A, Gareth N L, Ferrarelli T, Moger J, Schatzlein A G and Uchegbu I F: Delivery of Peptides to the Blood and Brain after oral uptake of Quaternary Ammonium Palmitoyl Glycol Chitosan Nanoparticles. Molecular Pharmaceutics 2012; 9: 1764-1774

4. Uchegbu I F, Sadiq L, Arastoo M, Gray A I, Wang W, Waigh R D, Schatzlein A G: Quaternary ammonium palmitoyl glycol chitosan- a new polysoap for drug delivery. International journal of pharmaceutics 2001; 224: 185-199

5. Siew A, Le H, Thiovolet M, Gellert P, Schatzlein A, Uchegbu I: Enhanced oral absorption of hydrophobic and hydrophilic drugs using quaternary ammonium glycol chitosan nanoparticles. Molecular pharmaceutics 2012; 9:14-28

6. Lalatsa A, Lee V, Malkinson P J, Zloh M, Schatzlein G A: A prodrug nanoparticle approach for the oral delivery of a hydrophilic peptide, leucine-enkephalin, to the brain. Molecular pharmaceutics 2012; 9:1665-1680

7. Garrett N L, Lalatsa A, Begley D, Mihoreanu L, Uchegbu I F, Schatzlein A G and Moger J: Label- free imaging of polymeric nanomedicines using coherent anti- stokes Raman scattering microscopy. Wiley online library 2012; 43: 681-688

8. Pillai C K S,Willi P, Chandra P S: Chitin and chitosan polymers: Chemistry, solubility and fiber formation. Progress in polymer science 2009; 34: 641-678

9. Prabaharan M, Mano F J: Chitosan-Based Particles as Controlled Drug Delivery Systems. Drug Delivery 2004; 12: 41-57

10. Uchegbu I F, Schatzlein A G, Tetley L, Gray I A, Sludden J, Siddique S and Mosha E: Polymeric Chitosan-based Vesicles for Drug Delivery. Journal of Pharmacy and Pharmacology 1998; 50: 453-458

11. Knight D K, Shapka N K, Amsden B G: Structure, depolymerisation and cytocompatibility evaluation of glycol chitosan. Wiley InterScience 2007, 787-798

12. Santiago de Alvarenga E: Biotechnology of polymers. InTech, 2011: 91-104

13. Alves N M and Mano J F: Chitosan derivatives obtained by chemical modifications for biomedical and environmental applications. International Journal of Biological Macromolecules 2008; 43: 401-414

14. Tommeraas K, Varum K M, Christensen B E and Smidsrod O: Preparation and characterization of oligosaccharides produced by nitrous acid depolymerisation of chitosan. Carbohydrate Research 2001; 333: 137-144

15. Qu X, Khutoryanskiy V V, Stewart A, Rahman S, Papahadjopoulos-Sternberg B, Dufes C, McCarthy D, Wilson G C, Lyons R, Carter C K, Schatzlein A and Uchegbu F I: Carbohydrate-Based Micelle Clusters Which Enhance Hydrophobic Drug Bioavailability by Up to 1 Order of Magnitude. 2006

16. Xia J, Song L X and Dang Z: Low-Temperature Carbonization and More Effective Degradation of Carbohydrates Induced by Ferric Trichloride. The Journal of Physical chemistry 2012; 116:7635-7643

17. Chang B L K, Tai M C and Cheng F H: Kinetics and Products of the Degradation of Chitosan by Hydrogen Peroxide. J. Agric. Food Chem. 2001; 49/10: 4845-4851

18. Fagerson I S: Thermal Degradation of Carbohydrates. J. Agric. Food Chem. 1969; 17/4: 747-750

19. Cabrera J C, Van Cutsem P: Preparation of chitooligosaccharides with degree of polymerization higher than 6 by acid or enzymatic degradation of chitosan. Biochemical Engineering Journal 2005; 25: 165–172

20. Nordtveit J R, Vårum M K, Smidsrød O: Degradation of partially *N*-acetylated chitosans with hen egg white and human lysozyme. Carbohydrate polymers 1996; 29/2: 163-167

21. Allan G G and Peyron M: Molecular weight manipulation of chitosan 1: kinetics of depolymerization by nitrous acid. Carbohydrate Research 1995; 277: 257-272

22. Allan G G and Peyron M: Molecular weight manipulation of chitosan 2: prediction and control of extent of depolymerisation by nitrous acid. Carbohydrate Research 1995; 277: 273-282

23.http://www.gelifesciences.com/gehcls_images/GELS/Related%20Content/Files/1314807262343/litdoc18102218_20131220222557.pdf

24. Aebersold R, Mann M: Mass spectrometry-based proteomicsm. Nature publishing group 2003; 422: 198-207

25. de Hoffman E, Stroobant V: Mass spectrometry: principles and applications, John Wiley & Sons 2007: 15-228

26. Council of Europe, European Pharmacopoeia Commission: European Pharmacopoeia 6.0, Conseil de l'Europe 2007: 228-230

27. Egerton R F: Physical principles of Electron Mycroscopy: An introduction to TEM, SEM and AEM, Springer 2006: 57-59

28. http://www.biophysics.bioc.cam.ac.uk/wp-content/uploads/2011/02/DLS_Terms_defined_Malvern.pdf

29.http://www.learningace.com/doc/2946038/fd53fbdf18aa5d00684292556af93695/zetasizer-chapter-16

30. http://golik.co.il/Data/ABasicGuidtoParticleCharacterization%282%29_1962085150.pdf

31. Goldburg W I: Dynamic light scattering. American journal of Physics 1999; 67: 1152-1160

32. Carneiro-da-Cunhaa G M, Cerqueirab A M, Souzab W S B, Teixeirab A J, Vicente A A: Influence of concentration, ionic strength and pH on zeta potential and mean hydrodynamic diameter of edible polysaccharide solutions envisaged for multinanolayered films production. Carbohydrate Polymers 2011; 85: 522–528

33. Salgin S, Salgin U and Bahadir S: Zeta Potentials and Isoelectric Points of Biomolecules: The Effects of Ion Types and Ionic Strengths. International Journal of Electrochemical Science 2012; 7: 12404 - 12414